Khanh Dao Le Cam

A Study of Open Circuit Voltage Production of Organic Photovoltaic Modules in the Outdoor Environment

Feathery Racades for Positive Energy Buildings Project (LIWEfacades project)

Metropolia
University of Applied Sciences

Author(s) Title	Khanh Dao Le Cam Environmental test of organic photovoltaic panels
Number of Pages Date	43 pages + 8 appendices 18 Apr 2019
Degree	Bachelor of Engineering
Degree Programme	Environmental Engineering
Specialization option	Renewable Engineering
Instructor(s)	Kari Salmi, Principal Lecturer, Smart and Clean Solutions

Organic photovoltaic modules printed by roll to roll technology is the resulting product of the Feathery facades for positive energy buildings project. It is demanding for the product to be tested before it can be manufactured in large scale and widely applied. This thesis is part of the project approaching the design of an outdoor testing system for the organic photovoltaics panels. The environmental variables of interest are irradiance, temperature, and humidity. The thesis aims to determine the dependencies of production of open circuit voltage on the environmental stress factor by implementing a test setup on four samples of organics photovoltaic panels.

The fundamental of organic photovoltaic cells and different testing techniques are briefly discussed in this thesis. The main focus is on illustrating the function of an outdoor testing system and the process of data analysis and interpretation. This thesis was written based upon the study of organic photovoltaics and the electrical component, in combination with the application of statistic, mathematics, and programming language.

The main finding determines a statistically significant effect of three dominant factors on open circuit voltage production of organic photovoltaics panels. In outdoor weathering condition, the dependency of open circuit voltage on surrounding factors is indicated to be similar to the previous research. However, it is ambiguous to give a conclusion in terms of how the impacts exerted on an individual device in the test.

Keywords	organic photovoltaics panel, outdoor test, ISOS census standard, environmental durability, Open Circuit Voltage

Metropolia
University of Applied Sciences

Acknowledgement

Contents

Metropolia
University of Applied Sciences

List of abbreviations and symbols

Al		Aluminum (cathode)
BHJ		Bulk-heterojunction
D.U.T	or	Devices under test
D_U_T		
FF		Fill factor
HOMO		Highest occupied molecular orbital
I_{SC}		Short – circuit current (A)
ISOS		International Summit on OPV Stability
ITO		Indium tin oxide (anode)
J_{SC}		Short – circuit current density (A/m^2)
LUMO		Lowest unoccupied molecular orbital
NOCT		Normal Operation Cell Temperature
OPV		Organic photovoltaic
OSCs		Organic solar cells
OTE		Outdoor Testing Environment
P3HT		Poly (3-hexylthiophene)
PCBM		[6,6] – phenyl – C_{61} – butyric acid methyl ester
PCE		photo – conversion efficiency
PCT		Percent
PEDOT: PSS		(poly (3,4 – ethylenedioxythiophene) polystyrene sulfonate)
PV		Photovoltaic
PVGIS		Photovoltaic Geographical Information System
R.H		Relative Humidity
Ref.		Reference
sufficient light condition		The condition with irradiation level between 80 mW/cm^2 to 110 mW/cm^2.
Temp.		Temperature
VIF		Variance Inflation Factor
VNC		Virtual Network Computing
V_{OC}		open – circuit voltage

1 Introduction

Through the last few decades, the increased living standard leads to the rapid development of infrastructure coupled with the energy demands for buildings. The traditional centralized energy supply is close to be overloaded; as a consequence, the localized energy production in combination with the conventional way of energy supply is the preferred solution in the future. One dominant way of localized energy production is integrated solar system, the silicon photovoltaics system, on the buildings' rooftop; yet, this solution remains with several barriers such as heavyweight, difficulty in installation, high overall cost. Subsequently, it is desirable to produce a new energy solution with more flexibility, lightweight, and lower total cost. [1.]

The Feathery facades for positive energy buildings project, or LIWEfacades for short, is initiated by VTT Technical Research Centre of Finland LTD to introduce a future solution for localized energy production in buildings. The principal idea is to fabricate light-weight solar panels which can be integrated into the building facade, in turn, leading to a zero-energy target. Furthermore, a positive energy building and wide-spread of off-grid energy production is not a far-fetched future. The LIWEfades project commenced in 2016, and the organic photovoltaics (OPV) panels are manufactured as a result of the research and development phase. Generally, the OPV cell is made from carbon and plastic which is promising to be a cost-effective way of generating electricity, in addition to its flexibility and significantly light-weight. [1.]

The OPV cell has not been dismissed because the challenges, i.e., its stability, power conversion efficiency remain unsolved. Thus, to deliver the OPV cell to end-use, it is required to test the OPV cell under various testing environment to ensure its quality. This thesis has been developed while working in the LIWEfacades project approaching the indoor and outdoor test. In this thesis, the main focus is the outdoor testing system, specifically, the design, function of the system, and the interpretation of the results. The outdoor testing system has not been completely developed to measure all the required variables by the time this thesis is written. Thus, the data analysis process indicated in this thesis covers a small scope in which the data can be interpreted. Specifically, open circuit voltage is the only photoelectric parameter to be measured together with two environmental factors including irradiance and temperature. The intricate dependencies

between OPV open circuit voltage with its influencing environment factor are expected to be the primary aspect to explore based upon the result of a previous experiment. [1.]

Among various environmental factors, there are three factors identified as the dominant variables to investigate in this thesis. Three stress factors include Irradiation, Relative Humidity, and Temperature. Based on the aim of the study, there are three main objectives defined for the thesis that corresponds to the answer to these following questions:

- Do all three environmental stress factors of interest (Irradiation, Relative Humidity, Temperature) have a statistically significant effect on the output open circuit voltage of OPV modules?

- If there is a significant impact, do the dependencies of open circuit voltage production on environmental stress factors follow a similar trend indicated in the previous study?

- If there is a considerable effect from an environmental factor, is the impact exerted equally on all modules?

The thesis consist of comprehends four main parts which are a literature review, methodology, result, and discussion. It provides a comprehensive review of operation and the impacts of environmental factors on open circuit voltage yielded by organic photovoltaic cells and its open circuit voltage production. In the methodology section, a complete view of the approach to thesis objectives and the transparent procedure to acquire and analyze data are presented. Thus, it is possible to carry out the repetition of this study, and the weakness of the system can be identified for further improvement. All the results and conclusions drawn in this thesis are entirely based on the analyzation of data set and interpretation based upon theory in previous researches.

Moreover, it should be noted that the terms *solar module* and *solar panel* are used to refer to a packaged, connected assembly of solar cells, and that both of the terms will be flexibly used in the text without any context-related differences in meaning.

2 Literature review

A more detailed account of organic photovoltaic technology is given in this chapter. First, the fundamentals of photovoltaic technologies are generally discussed, following a detailed description of the characteristics and operation of organic solar cells (OSCs). The second part of this chapter studies the degradation of OSCs, which also explains the motivation for the design of the experiment. A view of the relationship between open circuit voltage production and the dominant stress factor summarized from previous researches and books is provided as a basis to interpret the result of the data analysis process. The last part introduces various techniques to investigate the deterioration process of OSCs, and the principle of setting up an outdoor test.

2.1 Fundamentals of photovoltaic technologies

The general mechanism of the photovoltaic (PV) effect is the conversion of sunlight into electricity by PV cell. Photons, the component of the sun, are packed with solar energy; yet, the amount of energy contained these in photons are diverse in corresponding to different wavelengths of the solar spectrum. When hitting any object, the photons may pass through (transmission), be reflected (reflection) or be absorbed (absorption), only the absorbed photons can release the energy to the solar cell that generates electricity. [3.]

The relationship between the energy of a photon and the wavelength is shown in Equation 1 in which E is Energy of the photon, c is the speed of light equaled to $3x10^8$ m/s, h is Planck's constants equaled to $6,626x10^{-34}$ J.s, and lambda λ (m) is the wavelength.

$$E = \frac{hc}{\lambda} \tag{1}$$

The process of energy production starts when the energy of the photons is transferred to an electron in an atom of the semiconductor layer of a PV device. With enough activation energy, the electron escapes from its position and turns into a part of the electrical circuit. The PV cell is designated to have an internal electric field providing the voltage needed to drive the current through an external load. [3.]

The photovoltaic effect was discovered in the middle of the 18 century, but only until the early 1950s, the first viable PV cell was developed by Bell Laboratories Scientist. The arrival of the first PV cell placed a significant step toward the commercial market of PV. [3.] Currently, the dominant solar power solution comes from the conventional silicon PV cell. However, the downsides of this solution are the massive system which is not adaptive to a different building structure and the high installation cost which leads to high energy cost compared to the ordinary way of energy production using fossil fuels. Subsequently, a massive effort has been devoted to the research and development of alternative material and technologies to lower the overall cost and to improve flexibility. Mainly, organic photovoltaics (OPVs), or organic solar cells has drawn attention from scientists and investors due to its advantage of cost-effective, light-weight, simple fabrication process and flexibility. [4.] The next section describes the material, architecture, and operation of the OPV device in more detail.

2.2   Organic photovoltaics

An OPV cell is a class of solar cell in which organic materials are used for light absorption and charge transport. The discovery of conducting polymers by H. Shirakawa, Alan G. M. and Alan J. Heeger in 1977 altered the former perception that almost all organic compounds are inert for electrical conductivity, and enable a wide range of applications for the organic material, especially in PV cell production. [4, 5]

2.2.1   Material

In general, sp^2 hybridization occurs when an s-orbital of an atom mix with two other p orbitals; the results of the mixed orbital is called three sp^2 orbitals, in which the super-script indicate the number of orbitals of a specific type. When this three sp^2 orbital overlaps with appropriate orbital from another atom, the pi bonds (π-bonds) are formed. [7.]

Organic semiconductors are based on the conjugated polymer – a molecular entity whose structure has alternating single and multiple bonds between carbons atoms. In a conjugated polymer, the s and p orbitals of carbon atoms are hybridized and form the $3sp^2$ orbitals (σ-bond). The remaining fourth orbital pz from neighboring carbon atoms overlaps and forms the delocalized pi bond (π-bond). *Figure 1* is an example of σ-bond and π-bond.

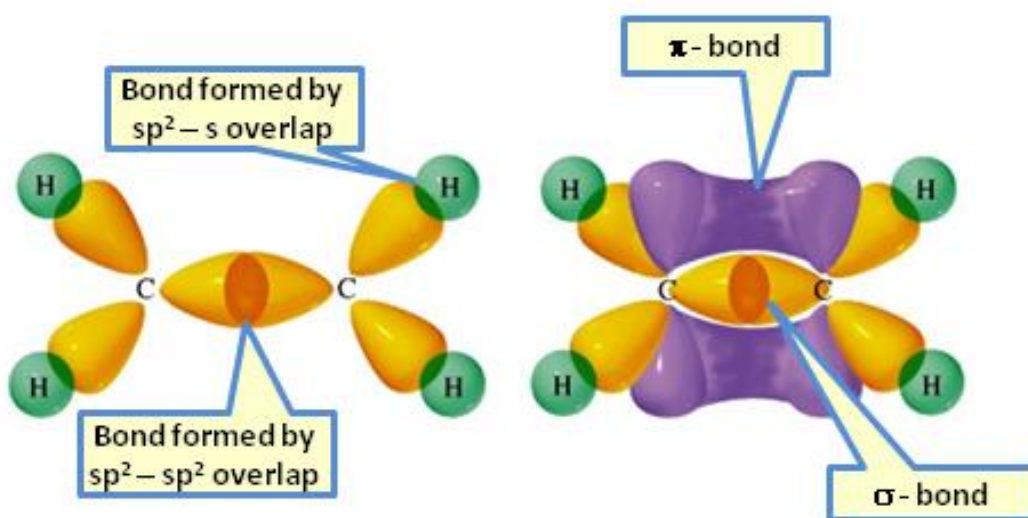Figure 1. π-bonds and σ-bonds [7]

According to Aufbau principle, the typical π-bond will have one π molecular orbital filled by electrons and one π molecular orbital with zero electrons which are called bonding (π orbital) and antibonding (π* orbital), respectively [8]. *Figure 2* is a diagram of 2 π molecular orbitals in a typical π-bond.
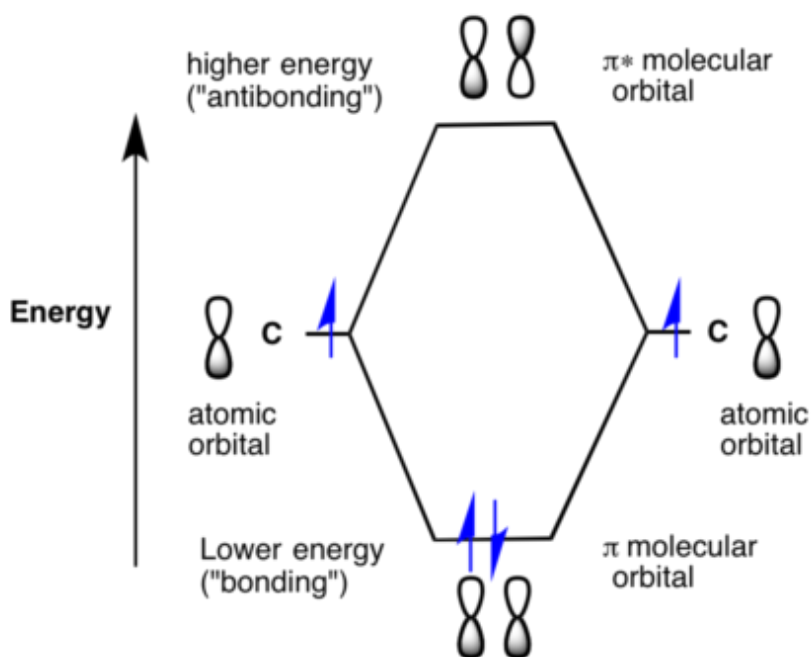

Figure 2. Bonding and antibonding in a typical π-bond. [8].

The bonding (π) and anti-bonding (π*) orbitals corresponds to the highest occupied molecular orbital (HOMO) and lowest unoccupied molecular orbital (LUMO) [4, 9]. In comparison to an ordinary inorganic semiconductor formed by joining a n-type material with high electron concentration and a p-type material with high hole concentration, LUMO is equivalent to the conducting band whereas HOMO is equivalent to the valence band. The reason to use the term HOMO and LUMO when referring to organic material is the electronic states in the polymer are not adequately dense to describe as bands. Thus, the use of molecular orbital draws a better approximation [10]. The bandgap of the organic polymer is yielded by the energy difference between HOMO and LUMO [4, 9]. The mobility of electrons in the π bonds – between the HOMO and LUMO band edge – shapes the semiconducting properties of conjugated polymers [11, 12]. In *Figure 3* P3HT, PE-DOT: PSS and PCBM are shown as a representative example of the most extensively investigated conjugated polymer used in OPV production.
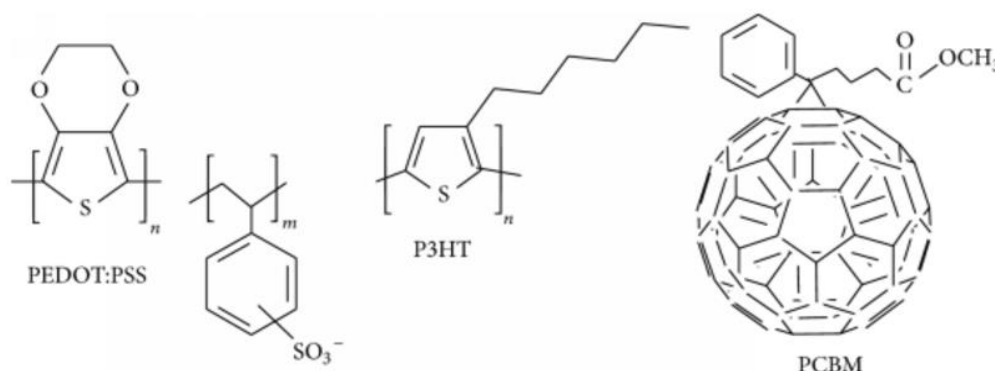
Figure 3. Most common conjugated polymers used in OPV production.[13]

2.2.2 Organic solar cell architectures

The first OSCs inherited the single layer structure consisting of an active layer placed between two electrodes. This type of OSCs has a relatively low efficiencies ranging from 0.0001 to 0.01 %. In late 1980s, the bilayer heterojunction OSCs is invented. In the bilayer structure, two organic material was laid on top of each other, in which the donor is the electron donating material, while the acceptor is the electron accepting material. The invention of bulk-heterojunction in later years had a significantly improved efficiency of OSCs. In the bulk-heterojunction solar cell, the donor material and the acceptor material are mixed forming a continuous, interpenetrating network in the active solar

layer. [8, 11, 12.] In *Figure 4*, a schematic of different OSCs architecture is illustrated, in which the arrows depict the pathway of charge transport to the electrodes. *Figure 5*, demonstrates the architecture of the tandem organic solar cell.
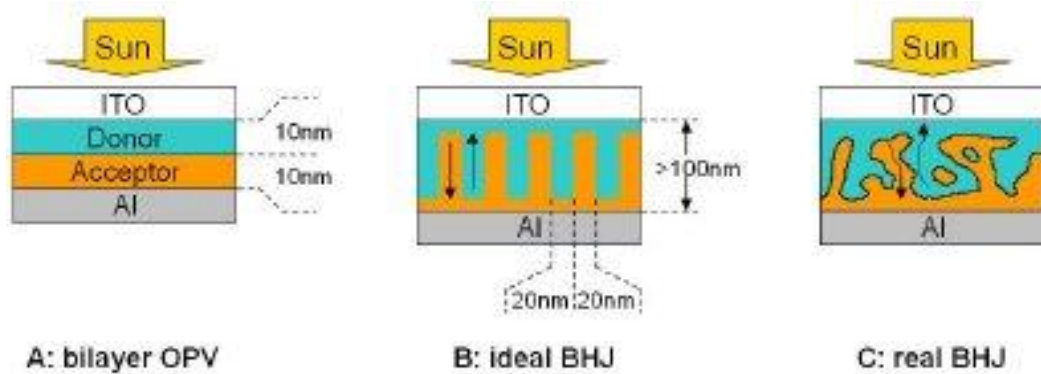
Figure 4. Scheme of the bilayer, ideal BHJ and actual BHJ OSCs [16]
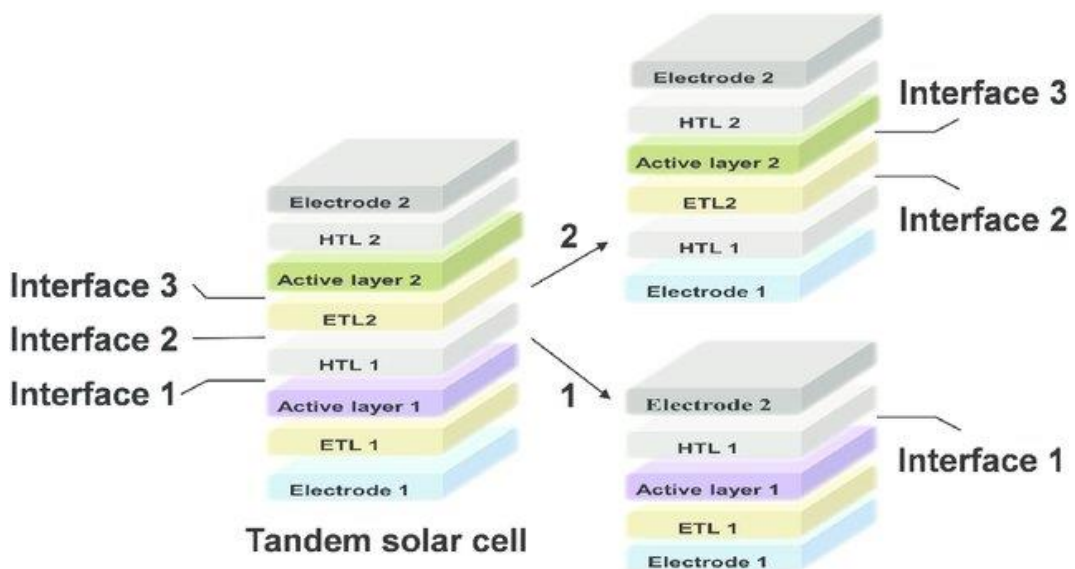
Figure 5. Architecture of Tandem organic solar cell.[17]

A further improvement, in terms of light absorption and the performance of OSCs, is shown in the Tandem Organic Solar Cells. The Tandem OSCs is formed by stacking two sub-cells together. With two different sub-cells, one has a wide bandgap, and the other has small bandgap active layer, the OSCs can absorb light over a broad solar spectrum [5, 19, 20]. Whereas, with a combination of two identical sub-cells will increase the light absorption within the same solar spectrum region. [4, 16–18.]

2.2.3   Organic solar cell mechanism

The active layer of OSCs, inheriting the p-n junction structure of the conventional PV cells, can be described as the combination of a p-type (electron donor, D) and a n-type (electron acceptor, A) material which is demonstrated in *Figure 6*. The p-n junction layer is sandwiched between a transparent anode, referred to as ITO, and a metallic cathode referred to like Al. *Figure 6* is the energy diagram of OSCs and the example of typical organic semiconductors. [13.]
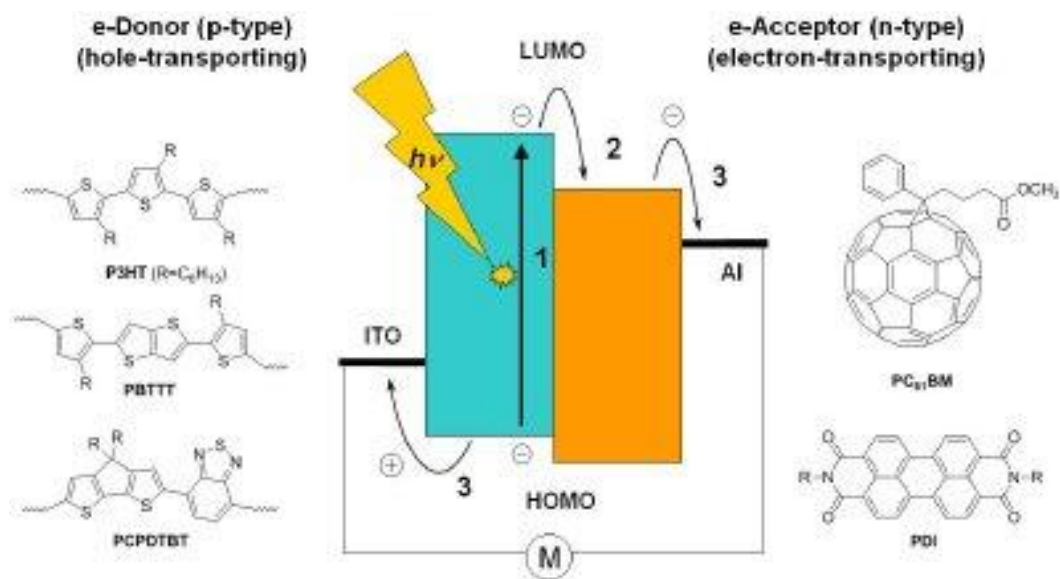
Figure 6. Energy diagram of OSCs. [16]

The absorption of photons from the incident light excites the electron in the donor material from its ground stage (HOMO) to the excited state (LUMO). Subsequently, electro-statically coupled electron-hole pairs, called exciton, are formed. Exciton is a neutral species that current cannot be generated from it. In π conjugated materials, the exciton has fairy high binding energy that first it has to be formed upon the photon absorption then it is dissociated to generate current. The exciton diffuses to the D-A interface, which is created by electronic interaction at the heterojunction, after that it undergoes a charge transfer to the reach the LUMO level of the acceptor. The electron released from the exciton is then transported to the electrode and recombination with the hole through the external circuit. This transportation of electron creates a photocurrent. [13.]

2.3 Degradation of the organic solar cell and testing techniques

One of the significant questions in the development of any PV is where stability or instability arises. The approach to the stability of solar cells by examining degradation is, in the scientific point of view, considered to be less complicated in both research and characterization process. The stability of solar cells can be classified into instinct stability and extinct stability; the former is rooted in the characteristic of the constituents, while the latter is linked to the broader connection within the solar cells. Therefore, it is essential to know whether the degradation is connected to the instinct or extinct stability that appropriate experiment can proceed toward either the fundamental material or the corrosion or formation of a crack that leads to failure in the operation of solar cells. [20.]

A stable solar cell, ideally, has consistent performance and appearance over time, despite the surrounding conditions that the cell is subjected to. For that reason, the environmental or surrounding conditions are often combined and employed to the design of an experiment in which the changes in the performance is deliberately observed. Implementation of the environmental test followed by an analysis can find the source of degradation, to rectify a particular degradation problem, the question of why and how the cell degrades need to be investigated. The intention of the test in the small scope of this thesis is to visualize the degradation of the OSCs, and partially indicate the correlation between the environmental condition and the degradation process.

2.3.1 Open circuit voltage of organic solar cells

Open circuit voltage is a crucial factor determining the device efficiency, which represents the maximum voltage of a solar cell can extract to an external circuit [22]. Although extensive studies have been devoted to studying each photoelectric parameter of OSCs, the open circuit voltage and its correlation remain ambiguous. This subsection provides a concise review of open circuit voltage in OSCs and highlights the knowledge retrieved from the scientific paper that is potentially applicable in the interpretation process of the experimental data. *Figure 7* portrays the factors influencing the open circuit voltage either directly or indirectly via their correlation.

Figure 7. Factors that affect the open circuit voltage.[22]

It is indispensable to centralize the study on one or a few factors so that the effect of each factor on V_{OC} is thoroughly investigated. Based on the enclosed scope of the thesis, this literature review presents three elements named: temperature, light intensity, and humidity.

Temperature

The V_{OC} of bulk heterojunction OSCs is claimed to have an inverse relationship with the ambient temperature, this phenomenon is mostly attributed to the temperature dependence of V_{OC}, and the correlation is considered to be linear. Additionally, the *Figure 8* obtained from various studies shown a deviation of the linear dependence of V_{OC} on the temperature at 200 K or lower. The cause of this deviation is experimentally tested and explained by the saturation of V_{OC} at low temperature. However, regarding the weathering test condition in this thesis, the lowest temperature points was -10°C equivalent to 263 K, which is far beyond the saturation point of V_{OC} that the disorder of V_{OC} at low temperature can be excluded. [24.]
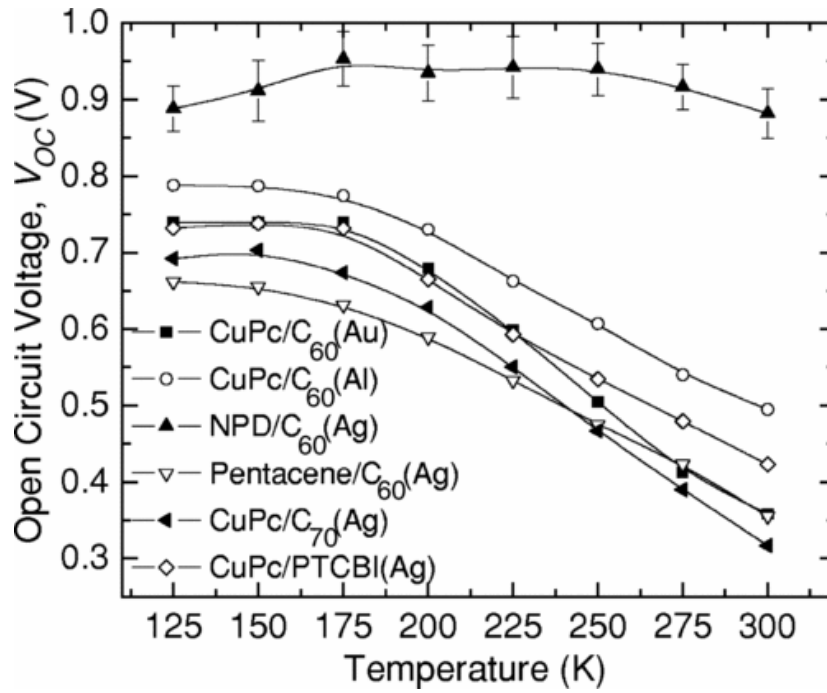
Figure 8. VOC versus T for various donor–acceptor heterojunctions. [23].

Figure 8 and Figure 9 reused with permission from the American Physical Society illustrates the intensity dependence of open circuit voltage.
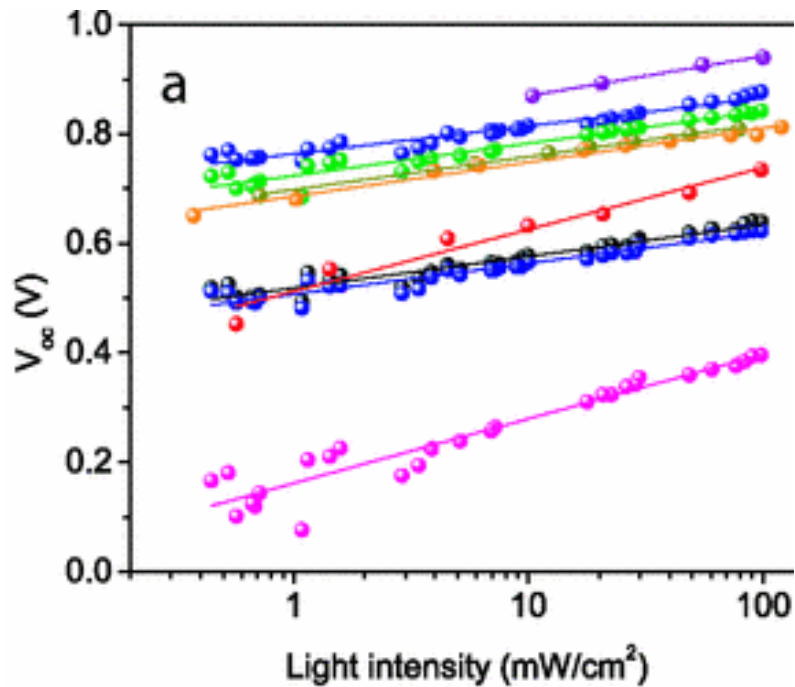

Figure 9. Light intensity dependence of V_{OC} where the photocurrent = 0.[24].

Humidity

The main effect of humidity on the OPV cell degradation is rooted in ambient oxygen and water which affects the stability of the device. The deterioration takes place when oxygen and water react, which leads to chemical degradation and photodegradation of the OSCs interfaces and organic layers. [27, 28.]

Light intensity

The exposure to irradiation of OPV cells prompts an arise of photodegradation in OPV cells. The OSCs inevitably operate under the light exposure, which means addressing the photodegradation issue is unquestionably a priority task. It is proven that OSCs are unstable during the exposure to irradiation; the exceptionally high light incident has been reported to severely deteriorate the OPV cells in about 100h of continuous exposure [27, 28]. The critical association between light exposure and OSCs instability is that irradiation triggers the photochemical and photophysical degradation occurring in every layer and interfaces of the devices [27, 29]. Photooxidation, arising as a consequence of light incident, impedes the operation of OSCs in several ways such as alternation of donor and acceptor structures results in decreasing the photoabsorption rate [27, 30].

Even though prolonged exposure to high light density can cause a severe impact on the operation of OSCs, this factor is coupled with the rise of open circuit voltage. Studies have shown that V_{OC} and light intensity (I) has a logarithm correlation depicted in *Figure 9* which means that the examined solar cell polymer, fullerene BHJ, δV_{OC} and ln(I) have the same slope.

2.3.2   Techniques to study the OPV degradation

General information about different testing techniques

The degradation of OPV can happen to a great extent, rooted from the inside of organic material to the deterioration of the complete devices affected by surrounding factors. In book named "Stability and Degradation of Organic and Polymer Solar Cells", the chapters 1 – 3 are dedicated to discuss in detail the equipment from Chemical and physical probes to the imagining technique used to study the deterioration occuring inside the organic material, whereas chapter 7 – 9 consist of the tests aimed at the

photoelectric performance, giving reflection of the complete device degradation. *Table 1* summaries different techniques that are currently available to apply in testing the OSCs.

Table 1. Different OPV degradation testing techniques.[21]

Degradation of organic material		
Physical Probes	UV-vis Spectroscopy	
	Atomic Force Microscopy (AFM)	
	Interference Microscopy	
	Scanning Electron Microscopy (SEM)	
	Light-Beam Induced-Current Microscopy (LBIC)	
	Electroluminescence and Photoluminescence Imaging Microscopy (ELI and PLI)	
	X-ray Reflectometry	
Chemical Probes	Infrared Spectroscopy (IR)	
	Time of Flight Secondary Ion Mass Spectrometry (TOF-SIMS)	
	X-ray Photoelectron Spectroscopy (XPS)	
Imaging techniques	Microscopy and Optical Scanning	
	Luminescence Imaging	
	Lock-In Thermography	
	Light-Beam Induced Current	
Degradation of the complete device		
	laboratory weathering testing	
	Laboratory Photoaging	
	Outdoor weathering	
	Concentrated light	

Outdoor weathering test

As was pointed out in the introduction chapter, this thesis is aimed at the behavior of OSCs corresponding to illumination, heating and humidify processes and the deterioration over some time. Therefore, this part describesthe instruments and tests targeting the photoelectric characteristic of the complete OCSs, as these factors are known as essential indicators of the OPV cell degradation process. Repeated measurement is accumulated and presented along the time axes to show the change in

the performance of the device by the time it is exposed to the environment condition. Primarily, the examination technique either gives information about one or all of photovoltaic properties including short circuit current, open – circuit voltage, fill factor, or photoconversion efficiency. The deterioration of OSCs can then be illustrated by plotting these above parameters against the time axes. The past researches and studies have found that environmental stress factors have significant influences on the photoelectric performance of OSCs; consequently, investigating in these factors also contributes to the study of degradation.

The International Summit on OPV Stability (ISOS) in the year of 2008 to 2010 provides in detail the procedures for testing the OSCs devices and modules regarding stability and operational lifetime. In terms of stability measurement, test protocols are divided into different categories including dark, outdoor, simulated light and stress testing, and thermal cycling. These tests have three levels of subtest: Basic (Level 1), Intermediate (Level 2), and Advanced (Level 3). The main parameters are similar for all categories (temperature, humidity, environment, light and electrical load); yet, the specific setup for each parameter is dissimilar. Three levels of outdoor testing specified in the article "Consensus stability testing protocols for organic photovoltaic materials and devices" published in *Solar Energy Materials& Solar Cells* journal is referred to in *Appendix II.*

A notable issue when conducting the outdoor measurement is the inconsistency between the irradiation level measured by a sensor and the actual irradiation received by a specimen at precise times of irradiation level. Instantaneous performance test need to be recorded and correlated. Additionally, it is required to obtain a continuous measurement of irradiation level to establish the total energy dose during the test of the specimen. The article "Consensus stability testing protocols for organic photovoltaic materials and devices" also recommended to avoid the non-linear effect; only the data measured in the irradiation ranging from 80 mW/cm^2 to 110 mW/cm^2 is taken into account when reporting the degradation curve. [21.]

Tilt angle

One factor that cannot be overlooked when designing a stationary solar cell test is the tilt angle. The tilt angle in a solar system is defined by the angle between the PV panel and horizontal surface; in other words, it is the angle at which the solar panels exposed to the sunlight. *Figure 10* is the illustration of the tilt angle in a static solar system.

Choosing a proper tilt angle is fundamental to a solar testing system as it exerts influence on the amount of solar radiation received by the device under test, in turn directly affecting the irradiance and temperature factor of the test. Additionally, the tilt angle assured the optimal amount of sunlight that reaches the solar panels varying according to a longitudinal and latitudinal location.
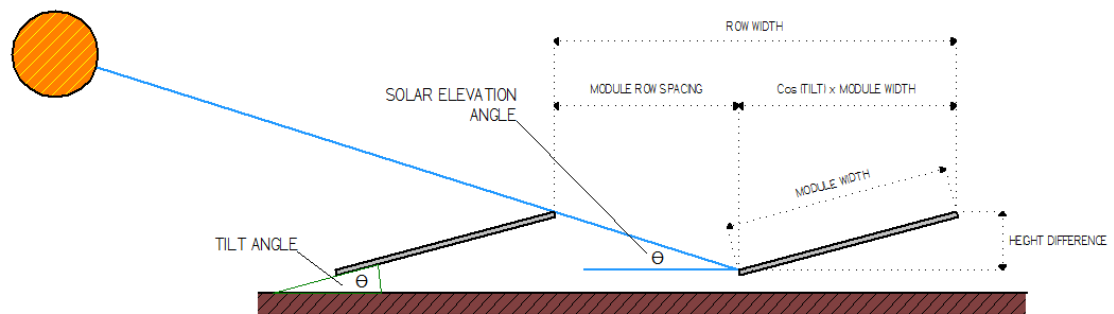
Figure 10.   Tilt angle and other factors of a solar system.[32]

The three ordinary exposure angels are 5º, 45º, 90º, which can be described as follows. At 5º tilt angle, the condensing water on the surface of the solar panel can drain off. At this angle, the solar panel can achieve the optimum of irradiance in comparison to other common angles; however, This only applies to the summertime, whereas in winter time, 5º tilt angle results in the lowest rate of receiving sunshine (compared to other common angles). 45º is a common tilt angle because 45º is the latitude angle of various US and European cities where exposures used in the past and continue to be applied until today. The 90º angle is mostly used when examining the condition on the façade.[20.]

In addition to defining a fixed tilt angle to receive an optimal amount of irradiance, a more advanced option is the sun trackers. The panels can be mounted to single-axis or dual-axis sun tracker that its angle will be altered corresponding to the sun position. In reality, this option is expensive and requires energy for its operation. Thus, it is more practical and applicable to orient the solar collector at an optimum tilt angle and to adjust the tilt correctly from time to time. [22.]

3   Methodology

This section gives a defined view of the method to approach the research problem and the procedure to work with the data. An in-depth description of the test setup, data collection, data manipulation, and data analysis is provided in this section coupled with a clear example of data and its change throughout the process.

3.1   Research method

Research method can be either quantitative or qualitative method, and it is critical to have a defined research method chosen logically based on the information type and analytical capability rather than intuitional decision [34]. Quantitative methods examine the measurable data whereas qualitative methods deal with non-numeric data. The modified data used in quantitative research consist of the following principal characteristics: measurable and numerical comparable. The conclusion established by quantitative analysis is statistically significant and representative for the whole population. The qualitative research methods implement a subjective point of view to study the behavior of a respondent group. In qualitative research, the variables are rather naturally observed than artificially controlled. The quantitative research methods are more frequently used technical fields, more specifically in the engineering field, as the nature of the data acquired in technological research.[34.]

The experiment design of quantitative method has two approaches which are deduction and induction. In the deduction approach, the starting point is a hypothesis based on theory; then, experiments are conducted to explore whether to confirm or reject the hypothesis. In contrast, the induction approach does not have any existing theoretical basis that investigation and observation is the initial step. If the outcome of the experiment is repeatable, a tentative hypothesis is formed, in turn, create a basis of a new theory. The former approach has an advantage that the experimental result is explainable with concrete theory prove provided that it has an appropriate context of rules and laws. However, there is no deviation for the outcome of a deductive test. On the other hand, the latter approach does contain room for deviation; albeit, the tentative hypothesis does not have actual proof until the theory is proven. For those reasons, neither of the procedure can have a perfect outcome, and it depends on the problems that the deductive or inductive approach will be more appropriate to be implemented. [34.]

The principle of this thesis is to statistically analyze the outdoor testing data and compare the trend with the prediction-based on theory. Hence, considering the goal and scope set for this thesis, the research method is classified to be a quantitative method in which an experiment is designed with numerically measurable data, the chosen approach is a deduction approach. *Figure 11* summarizes the methodological procedure that is taken into account in this study.
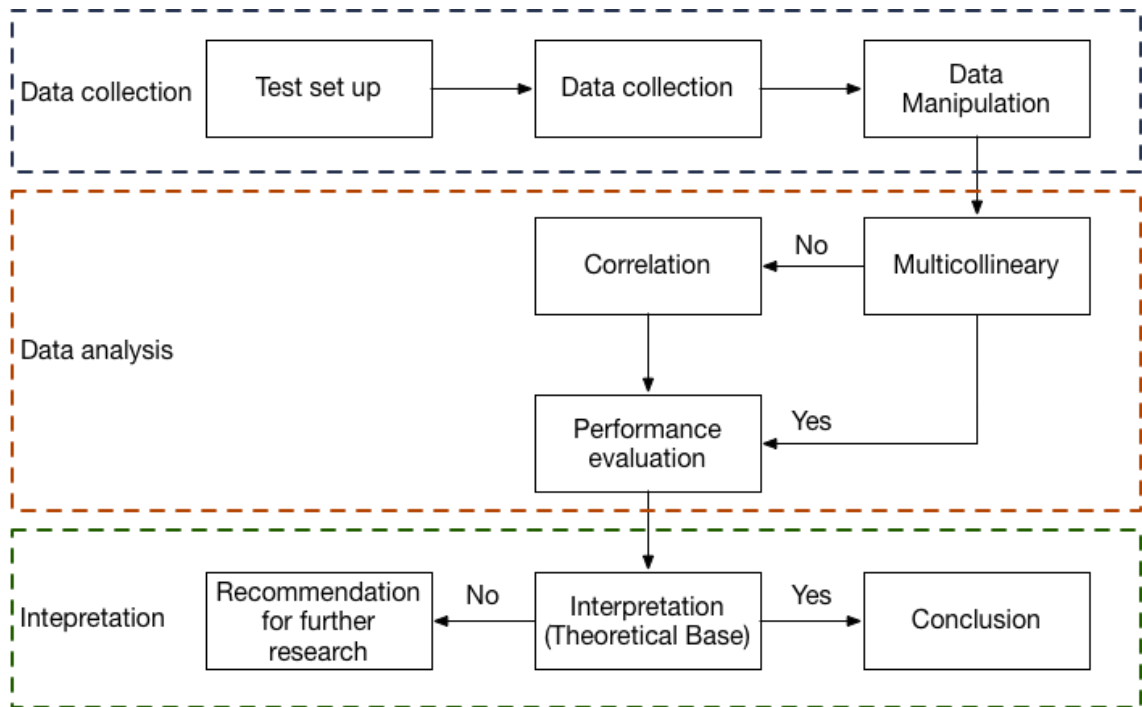
Figure 11.   Procedure diagram

In this study, there are three main steps in the research method including data collection, data Analysis, and interpretation. Initially, in the data collection step, a test setup that is suitable to examine the device is setup. After that, the data is collected, stored and manipulated so that it is ready to be utilized in the following process. Data analysis step commences with a multicollinear examination. If the cross effects of independent variables do not occur or occur in a small extent, the data can be transferred to the correlation test. Otherwise, it goes directly to the performance evaluation step. Then, the result is interpreted to see whether there is a theory that can explain the phenomenon. If the effect can be described according to academic studies, the conclusion can be drawn. On the other hand, if there is an inadequate theory available to interpret the experimental result, a recommendation for further research will be made.

Device under test

There are four solar modules of which general information of OSCs measured at infant stage is indicated in *Figure 12*, and *Table 2*.
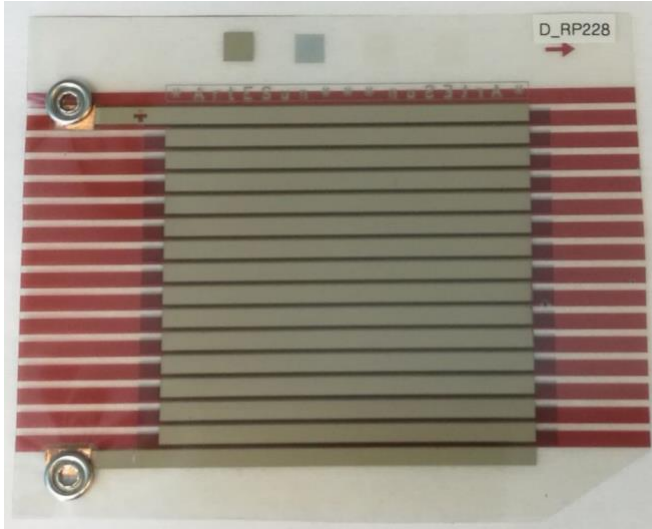
Figure 12.   Actual image of Roll to Roll printed organic solar module.[35]

Table 2 contains information of 4 solar modules named D_RP228, D_RP232, D_RP239, D_RP257, and these panels will be referred to as v1, v2, v3, v4 respectively. All the parameters were measured under solar simulator with 100 mW/cm2 intensity. I_{SC} and J_{SC} is current density, V_{OC} is open-circuit voltage, PCE is photoconversion efficiency. Copyrighted information is used with permission from VTT Technology Research Centre of Finland.

Table 2. Photoelectronic characteristic of OPV modules [35]

Module	ID	I_{SC} [A]	J_{SC} [A/m^2]	V_{OC} [V]	PCE [%]	Area [cm^2]
D_RP228	v1	-0.012	-0.661	8.460	2.474	18.00
D_RP232	v2	-0.012	-0.649	8.745	2.683	18.00
D_RP239	v3	-0.010	-0.563	7.141	1.362	18.00
D_RP257	v4	-0,012	-0.671	8.349	2.946	18.00

It can be seen from *Table 2* that the module named D_RP239 has a significantly less effective performance compared to the others as its PCE is approximately half of the other modules' PCE value. Additionally, in same light condition Module 1 and 2 are expected to have similar output and Module 4 is assumed to yield slightly higher output.

3.2   Data collection

The study is devoted to cover the study of open circuit voltage generated by OPV panels in an outdoor environment. This section provides a detailed description of the test setup to acquire data and the procedure to analyze data.

3.2.1   Test setup

The OSCs is connected to an open circuit, and the data is measured and monitored by the integration of microcontroller and a single portable computer system. *Figure 13* presents the equivalent circuit of one solar cell, which in reality is implemented on 4 OSCs. *Figure 13* is created on System Vision® Cloud. D_U_T is device under test, ADC depicts the microcontroller Arduino. R1 = 1,000,000 Ohm, R2 = 100,000 Ohm.
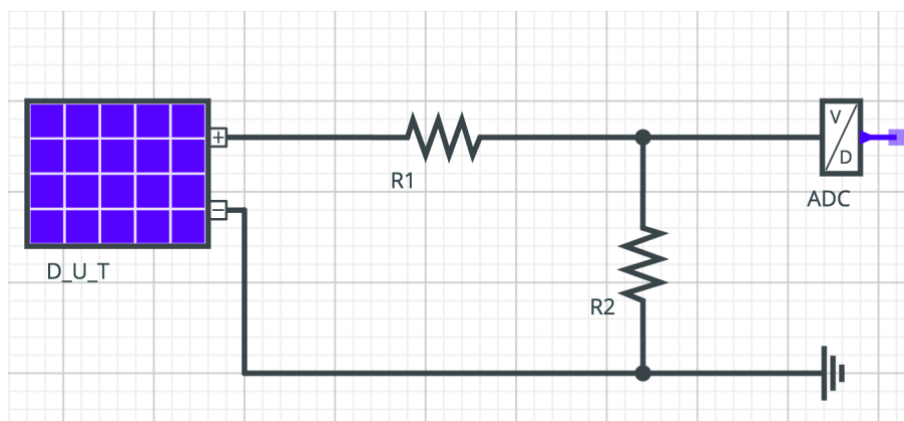
Figure 13.   The open circuit for a single solar cell.

The circuit acts as a voltage divider in which the positive terminal of the OPV cell is connected to a series of 2 resistors. The voltage read is located between R1 and R2. The microcontroller Arduino is only able to read the voltage in the range of 0 V to 5 V, whereas the standard voltage is measured to reach 8.7 V (*Table 2*) under sun simulator light in the laboratory. Hence, when testing the OSCs under actual sunlight which will yield much bigger V_{OC}, it is essential to use the voltage divider so that Arduino can read the voltage from solar panels.

The OTE cabin is located on the rooftop of B building of Myyrmäki campus – a campus in Vantaa of Metropolia University of Applied Sciences. The Photovoltaic Geographical

Information System (PVGIS) is an open data source which allows collecting the irradiance data which contribute to the chosen tilt angle of the OTE cabin. *Figure 14* plotted the solar irradiance at the testing location in the year 2015 and 2016. The selected angle irradiation is 90º, and the optimal angles irradiation of 2015 and 2016 are 46 and 47 degrees, respectively. Figure 14 shows clearly that at a 46±1 degree tilt angle, the solar cell can be guaranteed to have the highest incidence of light. Thus, the tilt angle for designing the cabin for the installation the OSCs chosen is 46±1 degree.

Figure 14.   Monthly solar irradiation estimates at different tilt angles. [36]

Table 3 is the summary of the outdoor testing which was implemented by the author. As stated in Acknowledgements, the outdoor testing cabin was designed by Zac Taylor while the author contributes more in data collection, data analysis, and interpretation parts.

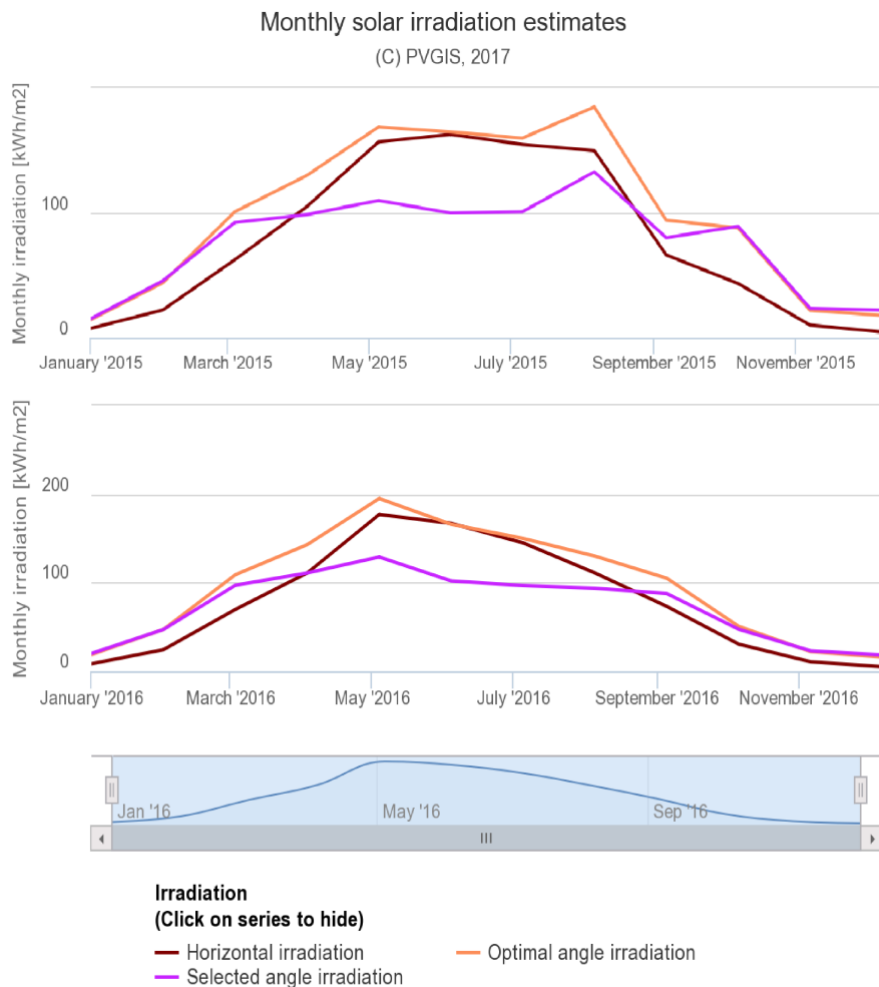Table 3. Outdoor testing specification [31]

Outdoor testing			
Test Setup		**Testing protocol**	
Light source	Direct sunlight	**Temp. /R.H.**	Monitor ambient values
Mounting	Static	**Solar irradiance (mW/cm²)**	Monitor irradiance and calculate accumulated irradiation
Load	Open circuit	**Measurement intervals**	1/15 minute – 1/1 hour
Temperature	Ambient	**Temp. ranges**	20±15°C
R.H.	Ambient		
Characterization light source	Outside under sunlight		

The test output reports the following values: date and time, ambient values of exposure Temp./R.H, open circuit voltage and sunlight irradiance. The open circuit voltage indicated the instantaneous performance and sunlight irradiance is the characterization light source.

In comparison to the test protocol provided in the ISOS, the applied setup can be considered to be in between the primary level and intermediate level. In contrast to the intermediate level setup (ISOS–O–2) which is fully referred in Appendix II, more frequent measurement and the direct measurement under sunlight will provide a data set with more precision and reduction of error due to the transportation of OSCs between extreme condition and laboratory condition.

The container of the outside cabin is made from transparent silicone with 4 OPV modules and the irradiation sensor placed in the front facing light source, Temperature, and R.H. sensors are located on the side of the cabin as indicated in *Figure 15*. Inside the cabin, there are 3 Arduino boards, a Wi-Fi router and a Raspberry Pi which are securely placed inside waterproof boxes. These container boxes (*Figure 15*) are specially designed and produced by 3D technology to achieve the 100% water proof environment for the electrical parts. The open circuit voltage of OPV modules and temperature were read by an Arduino whereas irradiation and humidity sensor is connected and read by separated Arduino board. The use of transparent plastic is a drawback of the cabin as when the system is placed under direct sun, not only the front surface is heated up but also the air and electronic parts inside the cabin are heated up. Therefore, the cabin has to be securely shielded to avoid water leaking into the electronic part; yet, on a dry and hot day; it needs to be open to reduce the heat accumulation inside the cabin.
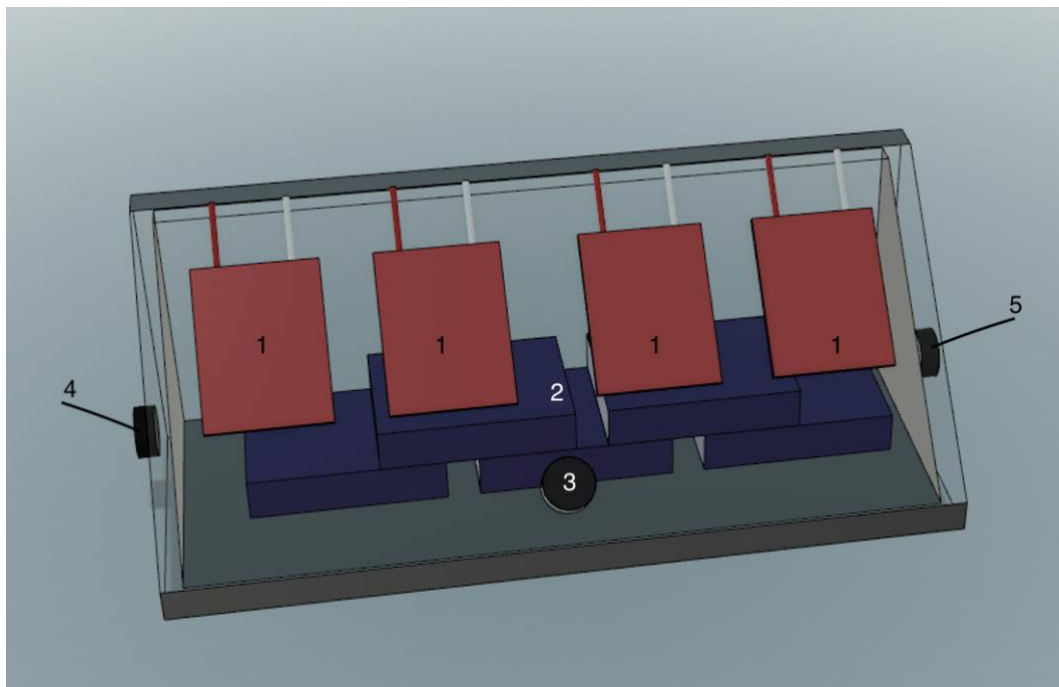
Figure 15.   Illustration of the outdoor testing cabin.

Figure 15 is the illustration of an outdoor testing cabin with transparent face holding the 4 solar modules; blue boxes are the containers for the electrical parts inside the cabin and the black part illustrates 3 sensors. The figure is created by Autodesk Fusion 360 student license.

1) Four OPV modules
2) Electrical parts enclosed inside waterproof boxes.
3) Irradiation sensor
4) Temperature sensor
5) R.H. sensor

Figure 16 shows that Raspberry Pi is a single-board computer which plays a central role in the data acquisition process. In the cabin, the Raspberry Pi provides power to Arduino and a Wi-Fi router, at the same time, it monitors the operation of Arduino by a python script and migrates the data to the cloud storage using internet connection. In general, the Raspberry Pi is set to operate automatically albeit with a virtual network computing (VNC) program that allows the external computer to manage the Raspberry Pi. VNC is a graphical desktop sharing system that enables an external computer to have access to the Raspberry Pi in case of maintenace for the remote system.
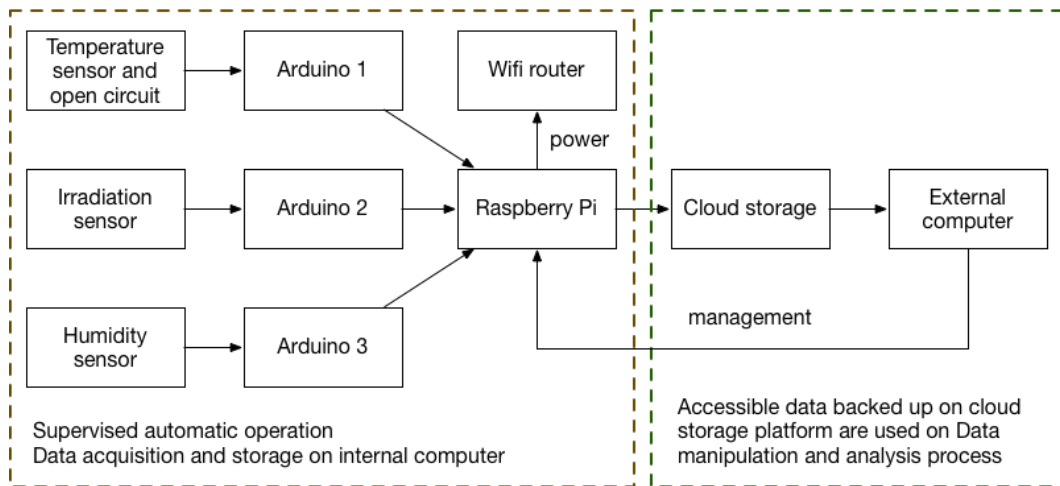
Figure 16.   Operation of the computing system diagram

Cloud storage system ensures the integrity, accessibility of the raw data regardless of any damage to the remote computing system might occur. Cloud storage is the single source of data implemented in further process on an external computer.

3.2.2 Data acquisition

Data collection process started on 2018-06-10 and ended on 2018-07-10 that the total duration was 30 days. The entire data acquisition is implemented by a remote system operate automatically under supervision of an external computer. Initially, the sensors are set to perform automatic measurement every second and micro-controller Arduino retrieved and read the measurement. Python script running by Raspberry Pi acquire the data from Arduino and written the measured values in raw data file imprinted with *a timestamp*. Each raw file is named after the type of measurement; for example, if the data is retrieved from Irradiation sensor, the file is named as *"IrradianceRAW.txt"*. Besides, every day the Raspberry Pi is set to run a python script that uploading all the raw data file on google clouds drive so that the data is safely stored and accessible for other purposes.

Due to the unique operation of each sensor referred to in the previous section, the test setup consists of three micro-controller units that builds three separate data files. *Figure 17* presents the data written in primary data files in which Voltage and Temperature, Irradiation and Humidity measurements are referred to as *VoltTempRAW.txt*, *IrradianceRAW.txt*, and *HumidityRAW.txt* respectively.

```
VoltTempRAW.txt
#Timestamp                      #Actual measured data
2018-06-18 12:23:38.150111,1.49,1.44,0.79,1.46,31.19
2018-06-18 12:23:49.279983,1.33,1.45,0.94,1.71,31.37
2018-06-18 12:24:00.419706,1.58,1.58,0.85,1.70,31.44
2018-06-18 12:24:10.544770,1.34,1.39,0.84,1.48,31.56
2018-06-18 12:24:21.679183,1.63,1.61,0.92,1.66,31.56


IrradianceRAW.txt
#Timestamp                      #Actual measured data
2018-06-18 12:23:56.370863,861.82 (W/m^2)
2018-06-18 12:23:56.368049,864.26 (W/m^2)
2018-06-18 12:23:57.382723,864.26 (W/m^2)
2018-06-18 12:23:57.380024,865.48 (W/m^2)
2018-06-18 12:23:58.394272,865.48 (W/m^2)


HumidityRAW.txt
#Timestamp                      #Actual measured data
2018-06-18 12:31:41.902459,22.78 (PCT)
2018-06-18 12:31:42.913684,22.93 (PCT)
2018-06-18 12:31:43.924533,23.22 (PCT)
2018-06-18 12:31:44.954289,23.07 (PCT)
2018-06-18 12:31:45.969951,22.93 (PCT)
2018-06-18 12:31:46.985407,23.07 (PCT)
```

Figure 17.   Raw Data file

The data transferred on the cloud drive was imprinted with *a timestamp*; the frequency of each measurement was somewhat different rooted in unique time index and a varied number of measures of each parameter. This problem is, in fact, indispensable as the reading speed of microcontroller varies and misread data occur uncontrollably. Hence, it is necessary to manipulate the raw data before it can be utilized.

3.2.3   Data manipulation

In the previous stage, the data is stocked up by the automated system, whereas the following processes are entirely performed on an external computer. After obtaining the full data set, the subsequent step is data manipulation that cleans the data and puts it in a standard form. The primary task that implements on all data file is to iterate through

the data and omit all misread data line resulted from the data acquisition process. There is the fact that the raw data imprinted with a *timestamp* in each primary file are different. *Figure 18* indicates a secondary data file that has a standard *timestamp*.

```
Line      Time stamp          v1,v2,v3,v4,Temperature
number

3744,    2018-06-18 11:49:00,14.19,14.22,12.24,15.4,29.11
3745,    2018-06-18 11:50:00,15.16,15.55,9.59,16.81,29.55
3746,    2018-06-18 11:51:00,16.04,15.9,13.75,16.81,30.16
3747,    2018-06-18 11:52:00,15.27,15.27,12.8,15.86,31.17
3748,    2018-06-18 11:53:00,15.53,15.62,13.84,16.72,31.86
3749,    2018-06-18 11:54:00,15.47,15.38,14.41,17.4,32.21

Line      Time stamp          Irradiation
number

3742,    2018-06-18 11:46:00,105.56
3743,    2018-06-18 11:47:00,104.42
3744,    2018-06-18 11:48:00,536.98
3745,    2018-06-18 11:49:00,740.91
3746,    2018-06-18 11:50:00,751.78

Line      Time stamp          Humidity
number

3742,    2018-06-18 11:46:00,35.41
3743,    2018-06-18 11:47:00,34.32
3744,    2018-06-18 11:48:00,30.02
3745,    2018-06-18 11:49:00,29.36
3746,    2018-06-18 11:50:00,29.44
```

Figure 18.   Manipulated data

As can be seen from *Figure 17*, voltage and temperature have the measurement written every 10 seconds, whereas, Irradiance and Humidity data appear almost every second. Hence, all measurements in a minute are averaged that create a stand *timestamp* for all the measurement consists of Date – Hour – minute – second, for instance, 2018-06-18 12:01:00 as illustrated in *Figure 18.* Beside the process implemented on all files, an additional process is performed on Voltage – Temperature raw data file. In *Figure 17*, the measured voltage has a magnitude of, for example, 1.49, 0.89 and 1.71 as the parameter was measured through a voltage divider circuit. The test setup in *Figure 13*

indicates two resistant values used to measure the open circuit voltage which is R1 = 10^6 Ohm and R2 = 10^5 Ohm. Therefore, to obtain the actual amount of open circuit voltage, Equation 2 is applied across the primary data of voltage.

$$V_{OC} = V_{measured} * R \tag{2}$$

$$R = \frac{R1 + R2}{R2} = \frac{10^6\ \Omega + 10^5\ \Omega}{10^5\ \Omega} = 11$$

On the basis of Equation 2 and the principle of test setup which allows the maximum value of 5 V to be measured, the optimal production of V_{OC} is 55 V. The data manipulation process generated 6 data files; three files contained measurements in June, and the other three contained measurements made in July.

3.3   Data analysis

After the manipulation process, all the data imprinted with the similar type of *timestamp* and data, it is convenient to combine individual file into a whole file by using the *timestamp* as an index for the merge. Python programming language, particularly the Pandas, Scipy and Matplotlib package, is implemented across this process. *Table 4* is extracted from the June data file in which each number presents the mean of all measurements within a minute, and all the figures were rounded to 2 decimals. v1 to v4 in *Table 3* refers to V_{OC} of OPV modules from 1 to 4.

Table 4. Example data after cleaning and structuring.

Index	v1	v2	v3	v4	Temp.	Irradiation	R.H.
2018-06-10 13:26:00	22.72	22.44	25.28	22.26	30.69	95.81	12.53
2018-06-10 13:27:00	22.20	21.65	25.21	22.07	30.29	95.64	12.79
2018-06-10 13:28:00	21.85	22.22	21.52	22.64	30.11	95.66	12.25
2018-06-10 13:29:00	21.91	21.85	22.97	21.71	29.67	95.78	12.28
2018-06-10 13:30:00	22.46	22.68	23.48	22.70	29.09	95.80	12.07
2018-06-10 13:31:00	22.99	22.96	22.19	22.52	28.47	95.10	11.69

It is important when analyzing the data that each variable is recorded in an appropriate form so that when it is passed to, for example, a regression model, the result makes sense both virtually and statistically. Initially, Irradiation data are stored as W/m^2 value in high light intensity conditions, its value might raise to approximately 1000. Other variables only vary in the range of 100 in which a maximum percentage of R.H. is 100%;

the highest ambient Temp. should not exceed 55°C, and V_{OC} cannot exceed 55 V. Consequently, The irradiation value needs to be conversed to a differently base unit that the value will vary in the range of 100. The new base unit was chosen for Irradiation in which 1 W/m^2 = 0.1 mW/cm^2. The outcome of unit conversion is illustrated in *Table 4.*

Tackling the first objectives of the study to explore how significant the effect of each environmental factor on the production of open circuit voltage, multiple regression was chosen to implement on the data set. However, the possibility of a cross effect between weathering factor might eliminate the meaning of regression method; therefore, the variance inflation factor (VIF) was also calculated. The outcome of VIF from each regression model of each module determines whether it is legitimate to study the regression model or not. There are two required criteria that need to be fulfilled before the investigation of correlation: the validation of the use of the regression model and statistically significant effects. If an environmental factor achieves these two criteria, its correlation with V_{OC} can be evaluated. If neither of the criteria is met, the correlation calculation process should not be performed.

The last process in data analysis is performance evaluation in which the output V_{OC} production needs to be vizualized on a scale so that the interpretation of the graph gives meaningful information such as maximum V_{OC}, a trend of the output V_{OC}, etc. Combination of all data file results in a data set with about 400,000 lines of record, in which each line contains a timestamp, voltage value, Temp. Irradiation ad Humidity. The main difficulty of this process is to identify a type of visualization that is fit for the vast number of data albeit with a bright display. Typically, a small data set with a few data points can easily be plotted on a scatterplot along a time series to illustrate its shape, trend, and projected the future development of the data. However, implemeting, for example, the scatterplot, line chart and box plot to visualize the enormous data set of this study did not appear to be a good visualization. Lastly, the violin plot was chosen to visualize the graph for evaluating the performance of the panels; scatterplot is also utilized; yet, with filtered data based on some specific criteria. Scatterplot visualization can be found in *Appendix II* and *Appendix III.*

4   Result and discussion

The photoelectronic characterizations measured at the early life of fourth OPV panels offer a basis to interpret the experimental data. At certain light intensity, Module 1 & 2 are projected to have similar electrical potential. Module 4 is predicted to yield the highest V_{OC} while Module 3 possibly has the least significant output. However, each module might react differently under varying weathering factors, in turn, the exposure to outdoor environment alters the optimal production extracted from each panel. The weight of each weathering factor and specification of how each of these factor impacts on OPV module is studied and interpreted in this section. On the basis of the reaction in the actual environment, the change in output V_{OC} can be explained in particular circumstance.

4.1   Multiple regression

Initially, multiple regression was used to create a prediction model for each of the module. The mathematical formula applied in the regression is Voc~irr+T+hum. The test is applied across the whole data set in which multicollinearity might occur due to various weather condition. Therefore, an additional calculation of the variance inflation factor (VIF) is conducted to detect the correlation between independent variables. *Table 5* shows summarized the regression results.

Table 5.   Multiple linear regression test result for Module 1-4

	ID	coefficient	Standard error	P > |t|	VIF
Intercept	1	12.7227	0.116	0.000	
Irradiation	1	0.0864	0.001	0.000	1.888
Temp.	1	-0.2119	0.003	0.000	2.430
R.H.	1	0.0270	0.001	0.000	2.363
Intercept	2	9.3847	0.091	0.000	
Irradiation	2	0.0662	0.001	0.000	1.888
Temp.	2	-0.1086	0.002	0.000	2.430
R.H.	2	0.0395	0.001	0.000	2.363
Intercept	3	8.2508	0.142	0.000	
Irradiation	3	0.1112	0.001	0.000	1.888
Temp.	3	-0.0176	0.003	0.000	2.430
R.H.	3	0.0109	0.001	0.000	2.363
Intercept	4	6.2409	0.151	0.000	
Irradiation	4	0.0992	0.001	0.000	1.888
Temp.	4	-0.0146	0.00	0.000	2.430
R.H.	4	0.0559	0.001	0.000	2.363

It is important to note that the regression is aimed to determine which variable has a notable influence on the dependent variable and the impact of one weather factor on the others is inevitable. For this reason, even though the VIF values in the range of 1 to 2.5 indicates a moderate correlation between independent variables, it is still acceptable to interpret the P-value and coefficient of this regression [37]. The p-value is less than the significant level (α) of 5% for all factors in the tests for four modules, which indicates that all three environmental factors have a statistically significant effect on the open circuit voltage of the OPV cell.

4.2   Correlation

In a general statistical method, correlation determines the degree to which two different variables are correlated; in this specific case , it was measured the correlation between open circuit voltage and one of the three environmental factors (Humidity, Irradiation, and Temperature). *Figure 19* depicts a guideline of correlation, albeit with no set values that demarcate, for instance from a strong to moderate correlation.
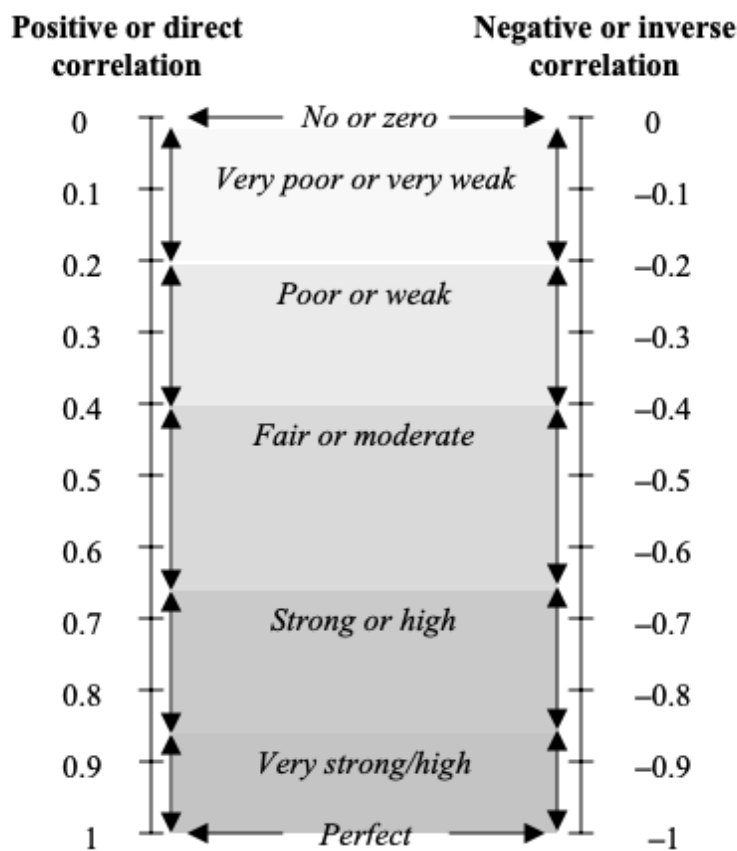

Figure 19.   Interpretation of correlation coefficient. Adopted from [38].

The association can vary from firm to weak or none (*Figure 19*), in which a strong correlation means that knowing the score of one variable can substantially predict the other variable. Regards less the strength of a correlation, positive (direct) correlation indicates that the higher the score of one variable the higher the score of the positively correlated variable. The negative (inverse) correlation means that if two variables have inverse trends; in other wordx, if one variable increases, the other variable will decrease.

Provided that the environmental variables are moderately correlated, the correlation of Temperature and R.H. versus V_{OC} is extracted at each irradiation range to minimize the correlation between these independent variables. The irradiation level is rounded up and and an irradiation index was set ranging from 0 to 120 mW/cm^2 with 10 mW/cm^2 interval. *Figure 20, Figure 21 and Figure 22* show the correlation of Irradiation Temperature, R.H. and V_{OC}, respectively.

4.2.1   Correlation of Irradiation and open circuit voltage

Figure 20 is the plot of irradiation index at a temperature index while additional visualization of output open circuit voltage versus light intensity is included in *Appendix IV*.

The numbers remain positive at the Temperature ranging from 0°C to 50°C, and reach the highest peak at 20°C, 30°C and 40°C ambient temperature for Module3, modules 1&2 and Module 4 respectively. From 0 to 10 figures of modules 1 and 4 undergo a decrease period, in contrast, the numbers of Modules 2 and 3 increase as the temperature increase. In extreme conditions above 50°C, the decline in correlation with Irradiation is observed in all modules.

The figures of modules 1 and 2 continue following a virtually similar trend; the data gradually grow as the temperature rises and peak at 30°C. Then this trend reverses; coupled with the increment of Temperature the figures slowly fall. At normal Temperature conditions ranging from 20°C to 40°C, the figure of Module 1 and Module 2 remain at about 0.6.

The figure of Module 3 increases dramatically when the Temperature range rises from 0 to 20 and reaches the highest peak of 0.9 at 20°C after that Module 3's number endures around 0.8. Above 10°C, the figure of Module 4 also increases gradually albeit with

slower pace compared to the figure of module 1 and 2. At normal ambient temperature range, the correlation coefficient of module 4 is approximately 0.6.
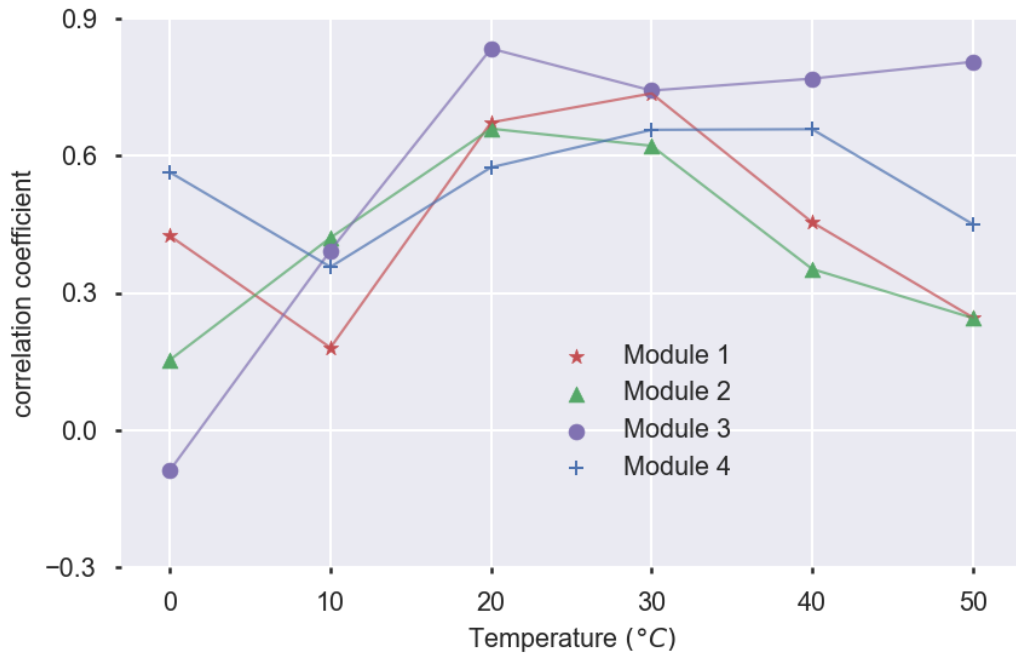

Figure 20.   Changes of Irradiation correlation coefficient at each Temperature index

Low temperature ($T \leq 0°C$) in the summer month of June and July typically coupled with low and unstable light intensity, hence the occurrence of the negative irradiation correlation coefficient in this condition is likely due to outlier data. Regardless of the abnormal irradiation correlation coefficient of module 3 at $T = 0°C$, the figures of all four modules are appeared to be positive. Thus, it means that light intensity has a positive effect on open circuit voltage yielded by OPV modules in an outdoor test condition. Additionally, observation shows that Module 3 has a strong correlation with irradiation.

4.2.2   Correlation between temperature and open circuit voltage

Figure 21 clearly shows that both Module 1 and Module 2 have almost identical Temperature correlation coefficient. Module 4's graph follows a similar trend; yet, the coefficient has a much smaller magnitude, whereas the figure for Module 3 is slightly different from the others. At the irradiation level below 80 mW/cm², the numbers of Modules 1 and 2 appeares to be negative and remains stable at about -0.6; above that irradiation level, it rapidly decreases.
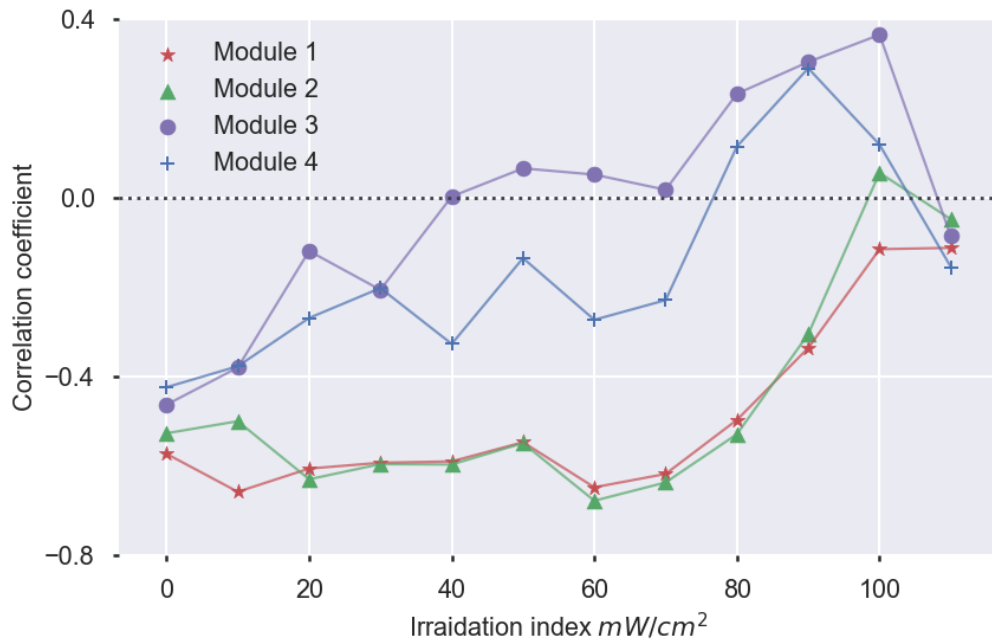
Figure 21.   Changes of Temperature correlation coefficient at each Irradiation index

In a low light intensity range below 80mW/cm^2, the higher the irradiation is, the smaller the figures of modules 3 & 4 and Temperature are. There is a difference between modules 3 and 4 despite the reduction, the number of Module 4 continues having negative value while Module 3's figure bottoms out at irradiation index of 40 and changes to a positive value. When irradiation reaches the sufficient level (>80 mW/cm^2), there is an observable increase in correlation between V_{OC} of Module 3 and 4 and Temperature.

The figures of all module drop rapidly at an extreme light intensity (>100 mW/cm^2). *Appendix III* contains additional plots of open circuit voltage versus Temperature at different irradiation index. The data points are scattered albeit with the black line represent the overall trend of the data.

Figure 21 shows that there is an apparent inverse correlation between ambient Temperature and V_{OC} output of modules 1 and 2, corresponding to studies referred to in literature review section (2.3.1). The figure of Module 4 presents a moderate negative correlation of Temperature and open circuit voltage at low light intensity number; however, at sufficient light condition, this correlation coefficient of Module 4 is altered to a positive value. The change in correlation coefficient derived from Module 4 data might have resulted from the stronger positive effect of irradiation at sufficient light condition accelerating the output open circuit voltage that suppresses the negative impact of

Temperature. Module 3 has a mere negative number of temperature correlation coefficient at irradiation index below 40, above that level, the temperature correlation coefficient of Module 3 is a positive number. Therefore, the figure illustrates a relatively weak correlation between temperature and output open circuit voltage, also, the increase of correlation coefficient at an adequate light condition projects that the influence of irradiation exerted on V_{OC} production of Module 3 outpower the effect of temperature in this circumstance.

In short, the temperature correlation coefficient of Modules 1 and 2 are predicted to persist with a similar trend compared to theoretical studies whereas the correlation of temperature and open circuit voltage Modules 3 and 4 are more or less a negative but it is rather weak and likely to be suppressed at a high light intensity condition.

4.2.3 Correlation of R.H. and open circuit voltage

It can be seen from *Figure 22* that overall three modules 1,2 & 4 have the V_{OC} positively correlated with R.H., albeit only R.H. correlation coefficient of module 4 drop notably at sufficient light ranging from 80 mW/cm^2 to 100 mW/cm^2.
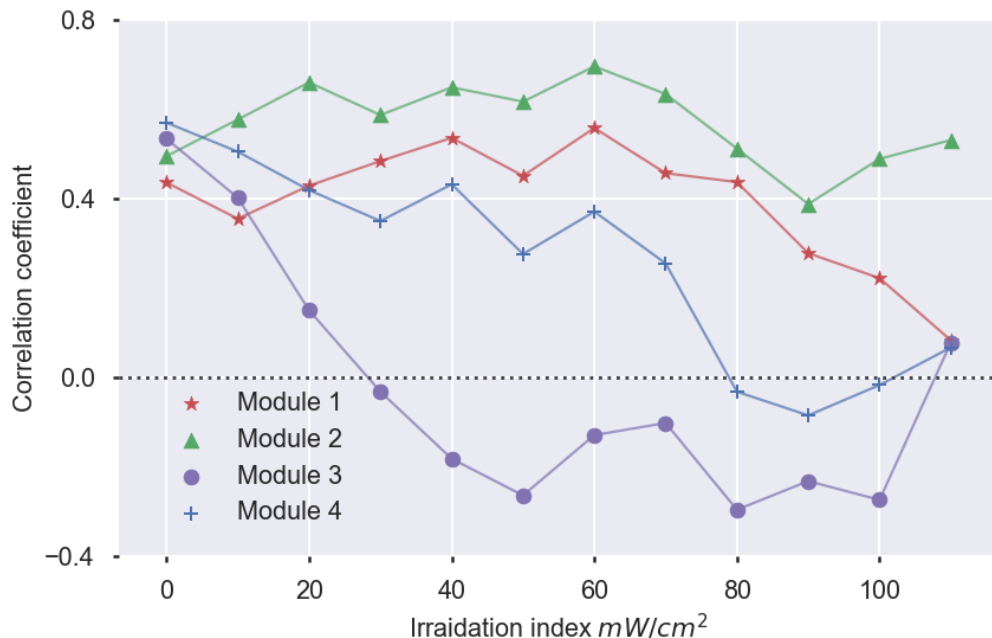

Figure 22.   Changes of R.H. correlation coefficient at each Irradiation index

The output figures of Modules 1 & 2 slightly fluctuate around 0.6 level at low irradiation level. In a sufficient light condition, the correlation coefficient of module 1 and module 2 experience a drop and a slight increment respectively while the figures remain with positive value.

Module 4 has a constant positive figure below the irradiation level of 70 mW/cm^2. Above that light intensity level, the graph representing V_{OC} – R.H. correlation of module 4 sinks significantly, and it remains merely above 0 in sufficient light condition. When irradiation level raises from 0 to 30, the figure of Module 3 drops remarkably and become a negative value at 30 mW/cm^2. The number slightly rises in the negative range and fluctuates around -0.3 point.

Figure 20 in section 4.2.1 shows that the open circuit voltage production of Module 3 has a strong correlation with light intensity, followed by a projection in part 4.2.2 that at sufficient light condition, the irradiation – V_{OC} correlation of Module 3 might be strong enough to suppress the effect of Temperature on V_{OC}. Nonetheless, in *Figure 22*, at irradiation index ranging from 40 to 100, the figure of Module 3 indicates a negative correlation coefficient. Thus, it is a likelihood that R.H. deploys a powerful influence on module 3 that the R.H. correlation of Module 3 constantly remains negative despite the strong positive correlation with irradiation might surge the V_{OC} output of Module 3. A similar scenario is predicted to apply on V_{OC} of Module 4 albeit with the effect of Irradiation and R.H. exerted on module 4 eliminating each other subsequently, the V_{OC} of Module 4 loosely correlate with R.H.

Table 6. Correlation summarization

	Irradiation	Temperature	R.H.
Module 1	Moderate to high positive correlation	Moderate negative correlation	Moderate to high positive correlation
Module 2	Moderate to high positive correlation	Moderate negative correlation	Moderate positive correlation
Module 3	Strong positive correlation	*Very poor negative correlation*	*Moderate to high negative correlation*
Module 4	Moderate to high positive correlation	*Very weak negative correlation*	*Weak to moderate positive correlation*

Table 6 tabulates the observed correlation and projected correlation of environmental factors and output open circuit voltage of each module, in which the assumption is presented by italic text.

4.3   Performance evaluation

Initially, the performance evaluation is expected to present in a line chart or scatterplot. A large number of data point coupled with outliners cannot be adequately illustrated by either line chart or scatterplot; therefore, a set of violin plots is applied to indicate the performance of 4 modules.

Part of the data in which light intensity is ranging from 80 mW/cm^2 to 110 mW/cm^2 is implemented in the assessment of OPV modules performance. V_{OC} outputs were continuously collated from June to July at an interval of 1 minute. The violin plots in *Figure 23* and *Figure 24* indicate the distribution of output V_{OC} from each module.

The former anticipation in section 6 is applicable for Module 1 & 2 as these modules yield an equivalent amount of voltage under the same condition. The outputs of these two modules distribute densely around 20 V level demonstrate consistent production of V_{OC}. The outliers occur more frequently in upper quantile indicates the ability to produce an open circuit voltage as high as 30 V. The observation of output V_{OC} distribution shows few outliers in lower quantile, this means that modules 1 and 2 indeed yield a small number of low open circuit voltage.

Module 4 has most of its data accumulated in the 18 V to 22 V range and the highest amount of voltage that can be yielded from this OPV module is approximately 33 V. The distribution of output open circuit voltage from module 4 has a higher density around the median compared to the figure of module 1 and 2. Coupled with a slightly higher median acquired *from Figure 23*, Module 4 is projected to yield better V_{OC} output in comparison to modules 1 and 2.
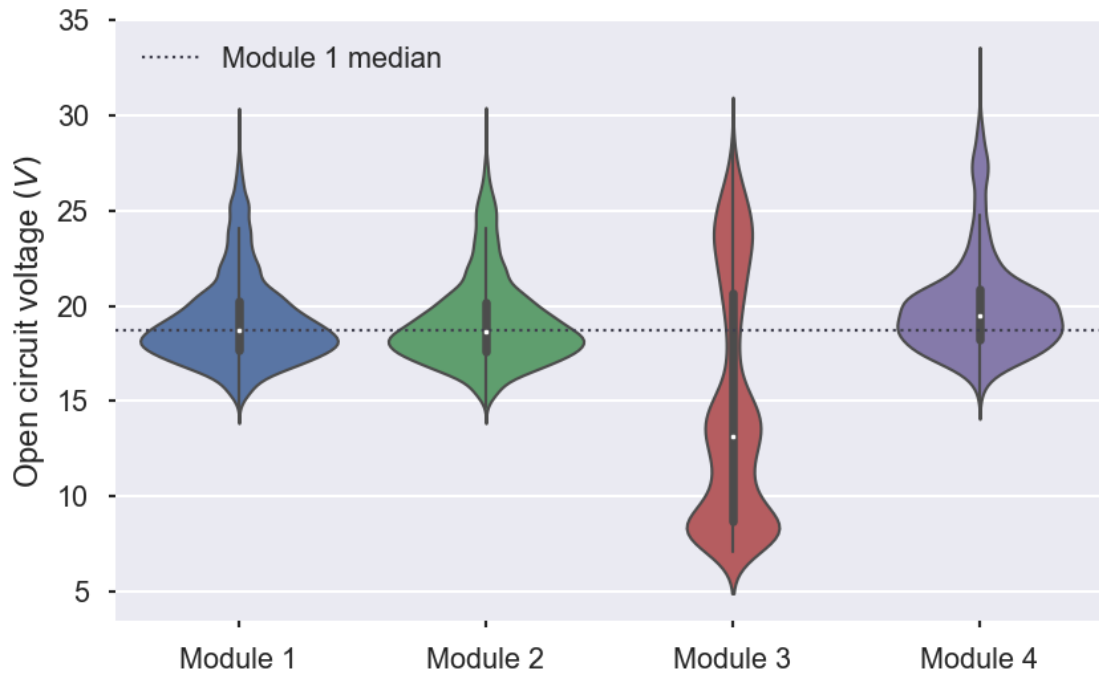
Figure 23.   Density plot of output open circuit voltage in June

Module 3 has an exceptionally different figure in which only extreme outputs occurs while the production in the normal range is absent. The data extracted from Module 3 forms higher density in lower quantile indicates that Module 3 mostly yield low open circuit output. The distribution of data point in upper quantile with smaller density shows that Module 3 can generate high V_{OC} output; yet, with low efficiency.

A horizontal line at the median value of Module 1 is placed in the plot to compare the overall performance of OPV panels. The experimentally calculated median of the first two modules is appeared to be equal; Module 4 has a slightly higher median, and Module 3 exhibits a modest median level. Module 4 can generate the highest V_{OC} output of 33 V. Modules 1 and 2 have consistent production around 20 V. Module 3 has low V_{OC} production; however, it is notable that this Module can generate high V_{OC} which is as high as 30 V. The confident interval of three Modules 1,2 and 4 are smaller than that of Module 3 which represent a more stable operation in terms of V_{OC} production of modules 1,2 and 4 compared to Module 3.

In July, modules 1 & 2 still have a steady performance, the V_{OC} produced by Module 3 declines significantly and more outliers recorded from Module 4. The notably smaller shape of the violin plots in *Figure 24* compared to *Figure 23* is due to fewer measurements were taken in July.
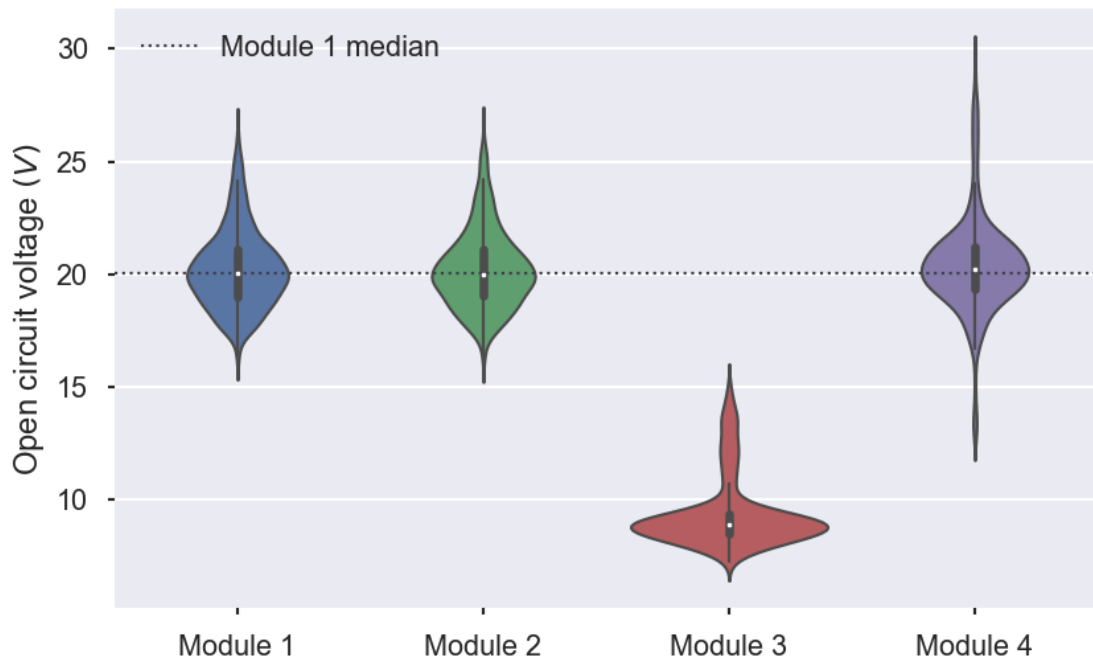
Figure 24.   Density plot of output open circuit voltage in July

From the July violin plots, Module 1 and Module 2 maintain a specific open circuit output around 20 V level that shows a constant performance of these two modules when exposed to similar conditions with other modules. The open circuit voltage yielded by Module 3 is low, and its highest peak is approximately equal to the lower limit of modules 1 and 2 confident intervals. Although it is observable that the data points in Module 4's figure distributes more densely around the median, it can be seen that more outliers occurs in Module 4 violin plot in July. Thus, this indicates a reduction in the efficiency of open voltage production of Module 4. From these observations, it is highly likely that Module 3 and 4 suffer more from the deteriorating process arisen from weathering exposure, in contrast, Module 1 and 2 might be less affected by the degradation resulting from environmental factors.

5   Conclusions

The research problem of the LIWEfacades was to explore the range and nature of influences from three environmental factors on organic photovoltaic panels provided by the VTT Technical Research Center. The thesis is devoted to covering a part of the project in which the investigation of dependencies between the open circuit voltageamd the weathering factor is performed. Three main environmental factors of interest were identified as Irradiation, Temperature, and Relative Humidity. There were three objectives of this study which were determined and explained in three sections of the data interpretation and analysis. Firstly, the data were investigated to validate whether three environmental factorswould have a statistically significant effect on the open circuit voltage production of four OPV modules tested. Secondly, the data set was inspected and visualized to evaluate whether it demonstrated a similar trend in comparison to the projected direction indicated in previous studies of open circuit voltage. Lastly, if previous phases substantiated the significant effect of environmental factors on open circuit voltage of OPV modules, it was studied whether the forces equally exerted on four devices under test.

A deductive quantitative research approach was adopted using a test setup following the ISOS (International Summit on OPV Stability) consensus standard derived for data acquisition and statistical methods to analyze and interpret the data. The influences of three weathering factors identified in the experiment studies were not discrete albeit with a moderate level of correlation between these factors. Thus, the regression method was implemented to study the retrieved data from each module. Investigation of P-value in regression established a statistically significant effect of Irradiation, Temperature and Relative Humidity on the open circuit voltage of all OPV panels.

To verify the impact of individual factor (Irradiation, Temperature or R.H.) on OPV open circuit voltage in controlled laboratory condition, the correlation between open circuit voltage and each environmental element was performed to determine whether the open circuit voltage persisted with a similar trend in varying weather conditions. The studies summarized in the book Stability and Degradation of Organic and Polymer Solar Cells by Frederik Krebs [21] and the article "Fundamentals of bulk heterojunction organic solar cells" by Rafique S, Abdullah SM, Sulaiman K, et al. [27] determine that all environmental factors trigger the deterioration of OSCs; yet, each element corresponds differently to the magnitude of output open circuit voltage. These studies also showed that Irradiation

exerts a positive effect on V_{OC} whereas, Temperature has an inverse impact on V_{OC}. In other words, the rise of light intensity aids the increment of output V_{OC}, and the temperature increase leads to a decline in the yielded V_{OC}. Besides, the theoretical studies also prove that there is a link between R.H. and the degradation of OSCs. However, the complex relationship between this environmental factor and open circuit voltage is not cited. Therefore, it is projected that exposure to R.H. over some time drive the degradation of OSCs, in turn leading to a reduction in V_{OC} output.

In the study of this thesis, the correlation figure derived from experimental data indicates that all four OPV modules more or less follow a similar correlation of Irradiation – V_{OC} and Temperature - V_{OC} in comparison to previous studies. The output open circuit voltage from these panels has a positive correlation with Irradiation and negative correlation with Temperature even though the correlation coefficient varies for each module. There is a slightly difference shown when collate the correlations between R.H. and V_{OC} production by each OPV modules since there is an inadequate theoretical basis to inteprete the phenomena. The analysis of the experimental data obtained in this study suggested that V_{OC} of Module 1,2 and 4 have positive correlation to R.H., whereas V_{OC} of Module 3 is predicted to have a strong negative correlation with R.H. The prediction should not be interpreted as a causation of Module 3's dissimilar result since it is only based on virtual observation of correlation coefficient. Nevertheless, it is possible to carry out further studies endeavored to explain the connection between R.H. and open circuit voltage of OPV modules.

A performance evaluation for each OPV module was approached by visualizing the data distribution on a violin plot in which only the data derived from measurements under sufficient light conditions is included. The result of this approach demonstrates the ability of the devices tested to yield high output open circuit voltage and assesses the stability in operation. Modules 1 and 2 can produce an output V_{OC} as high as 30 V, while V_{OC} production of modules 3 and 4 is 31 V and 33 V, respectively. In regards to V_{OC} production, the three modules 1,2 and 4 are observed to have stable performance, whereas the output from Module 3 varies significantly.

Furthermore, there is evidence of degradation observed from violin plots of modules 3 and 4 between June and July, while there is merely change in the figures of modules 1 and 2. Experiments clearly shown the number of modules 1 and 2 follow the theoretical basis with no strange figure appeared. The resulting figures of modules 3 and 4 are

relatively different from the first two modules especially in the correlation with R.H. part. Supposed that modules 1 and 2 exhibit correlation with environmental factors similar to that indicated in theory, and the causation of a slightly decreased output open circuit voltage is explainable by the deterioration resulted from a period of exposure to an outdoor environment. On the other hand, Modules 3 and 4 have a similar correlation with Irradiation, a loose connection with Temperature and a projected high correlation with R.H. The distribution plots of these two figures suffer from a significant change after a period of exposure to the outdoor environment. The rapid change in overall output V_{OC} yield by Modules 3 and 4 is possibly rooted in the excessive effect of R.H. on these panels that accelerated the degradation period. However, to firmly validate this hypothesis, a complete test covers all photoelectric parameters, and a physical examination of internal material degradation is required.

To sum up, initially, this thesis has successfully examined and determined that the environmental factors have a statistically significant effect on the output open circuit voltage of OPV panels tested. Secondly, the approach to correlation coefficient provides a vivid comparison between the theoretical and experimental correlation of open circuit voltage yield by OSCs and environmental factors. Last but not the least, this study strived to examine the weight of effect from each environmental factor on an individual module to explore whether the impact is equally exerted on all devices tested; however, it is ambiguous to give any conclusion in this perspective as there is a mere number of supporting evidence.

The primary difficulty of this study is the lack of general theoretical research that can explain intricate dependencies of open circuit voltage and the environmental factors. The individual effect of each weather factor in controlled condition was thoroughly investigated; yet, how the accumulative impact of two factors might alter the influences has not been demonstrated in any study and research in the past. The second obstacle is the test was setup with an unnecessary small measurement interval of once every 10 seconds which is too frequent compared to the suggested interval of once every 15 minutes in the advanced level of ISOS test setup. Small measurement interval caused numerous errors in reading, transferring and writing data of the microcontroller Arduino. Hence, it took a considerable amount of time to omit all the mistakes that occur due to fault in the operation of the computer system and the error data written in the data file. In the end, these obstacles were successfully tackled so that the study could optimize the use of retrieved data and the past research and study of open circuit voltage and

endeavor to interpret the result to a level that there are adequate evidence and theory available. Furthermore, considering a broader scope; a weakness remains in this project: the lack of multidisciplinary cooperation due to which the setup failed to measure both of the dominant photoelectric parameters.

In conclusion, the author had successfully overcome the obstacles at the beginning of the project to rapidly adopt the core idea and operation of test so that the study could be conducted and valuable results could be drawn after time and effort were devoted to investigating the research problem. Although the finding of this study is relatively general, it mainly supports the basis of studying complex characteristics of open circuit voltage in OPV modules. Moreover, various projections were demonstrated in this thesis so that based on them further study and research can be performed.

6   References

1   Tapio R, Sanna P, Päövi A, et al. *Feathery façades for positive energy buildings*. 2016.

2   Cook AG, Billman L, Adcock R. Photovoltaic Fundamentals. *J Plast Surg Hand Surg* 2014; 48: 96.

3   Wu B, Mathews N, Sum TC (Tze-C. *Plasmonic organic solar cells : charge generation and recombination*. 2016. Epub ahead of print 2016. DOI: 10.1007/978-981-10-2021-6.

4   Vivek K a, Agrawal GD. Organic Solar Cells : Principles , Mechanism and Recent Dvelopments. *Int J Res Eng Technol* 2014; 3: 2319–2322.

5   Shirakawa H, J. Louis E, G. MacDiarmid A, et al. Synthesis of Electrically Conducting Organic Polymers: Halogen Derivatives of Polyacetylene, (CH) X. *J Chem Soc Chem Commun*; 1977.

6   Bonding C. Curriculum Module : Chemical Bonding.

7   Organic semiconductors - Organic Electronics @IC Packaging Lab, https://oelectronics.weebly.com/organic-semiconductors.html (accessed 30 November 2018).

8   Molecular Orbital Diagram For A Simple Pi Bond – Bonding And Antibonding — Master Organic Chemistry, https://www.masterorganicchemistry.com/2017/02/14/molecular-orbital-pi-bond/ (accessed 2 December 2018).

9   Deibel C, Dyakonov V. Polymer-Fullerene Bulk Heterojunction Solar Cells. *Reports Prog Phys*; 73.

10   Schroeder R. Characterization of Organic and Inorganic Optoelectronic Semiconductor Devices Using Advanced Spectroscopic Methods. 2001; 135.

11   Kopola) PA (formerly. *Roll-to-roll printing of organic photovoltaic cells and modules Roll-to-roll printing of organic photovoltaic cells and modules*. University of Oulu, 2015.

12   Klauk H. *Organic Electronics II: More Materials and Applications*. Wiley-VCH. Epub ahead of print 2012. DOI: 10.1002/9783527640218.

13   Iwan A, Boharewicz B, Tazbir I, et al. Silver nanoparticles in PEDOT:PSS layer for polymer solar cell application. *Int J Photoenergy* 2015; 2015: 1–9.

14   Tang CW. Two-layer organic photovoltaic cell. *Appl Phys Lett* 1986; 48: 183–185.

15   Chamberlain G. Chamberlain, G.A.: Organic solar cells: a review. Sol. Cells 8, 47-83. *Sol Cells* 1983; 8: 47–83.

16   Flagship FM, Scientific C. Fabrication of Organic Photovoltaic Devices. 2009; 1–4.

17   Du X, Lytken O, Killian M, et al. Overcoming Interfacial Losses in Solution-Processed Organic Multi-Junction Solar Cells. *Adv Energy Mater*; 7.

18   You J, Chen CC, Hong Z, et al. 10.2% power conversion efficiency polymer tandem solar cells consisting of two identical sub-cells. *Adv Mater* 2013; 25: 3973–3978.

19   Sun X, Zhao D, Ke L, et al. Inverted tandem organic solar cells with a MoO3/Ag/Al/Ca intermediate layer. *Appl Phys Lett* 2010; 97: 53303.

20   Kim HP, Yusoff ARBM, Kim HM, et al. Inverted organic photovoltaic device with a new electron transport layer. *Nanoscale Res Lett* 2014; 9: 150.

21   Krebs FC. *Stability and Degradation of Organic and Polymer Solar Cells*. Hoboken, UNITED KINGDOM: John Wiley & Sons, Incorporated, http://ebookcentral.proquest.com/lib/metropolia-ebooks/detail.action?docID=887260 (2012).

22   Elumalai NK, Uddin A. Open circuit voltage of organic solar cells: An in-depth review. *Energy Environ Sci*; 9.

23   Rand BP, Burk DP, Forrest SR. Offset energies at organic semiconductor heterojunctions and their influence on the open-circuit voltage of thin-film solar cells. *Phys Rev B - Condens Matter Mater Phys* 2007; 75: 115327.

24   Cowan SR, Roy A, Heeger AJ. Recombination in polymer-fullerene bulk heterojunction solar cells. *Phys Rev B* 2010; 82: 245207.

25   Jørgensen M, Norrman K, Gevorgyan SA, et al. Stability of Polymer Solar Cells. *Adv Mater* 2011; 24: 580–612.

26   Grossiord N, Kroon JM, Andriessen R, et al. Degradation mechanisms in organic photovoltaic devices. *Org Electron* 2012; 13: 432–456.

27   Rafique S, Abdullah SM, Sulaiman K, et al. Fundamentals of bulk heterojunction organic solar cells: An overview of stability/degradation issues and strategies for improvement. *Renew Sustain Energy Rev* 2018; 84: 43–53.

28   Yamanari T, Ogo H, Taima T, et al. *Photo-degradation and its recovery by thermal annealing in polymer-based organic solar cells*. 2010. Epub ahead of print 1 June 2010. DOI: 10.1109/PVSC.2010.5616522.

29   Cheng P, Zhan X. Stability of organic solar cells: challenges and strategies. *Chem Soc Rev* 2016; 45: 2544–2582.

30   Deschler F, De Sio A, von Hauff E, et al. The Effect of Ageing on Exciton Dynamics, Charge Separation, and Recombination in P3HT/PCBM Photovoltaic Blends. *Adv Funct Mater*; 22: 1461–1469.

31   Reese MO, Gevorgyan SA, Jørgensen M, et al. Consensus stability testing protocols for organic photovoltaic materials and devices. *Sol Energy Mater Sol Cells* 2011; 95: 1253–1267.

32   Solar Shading Calculator | CivicSolar, https://www.civicsolar.com/support/installer/articles/determining-module-inter-row-spacing (accessed 2 December 2018).

33   Zang H, Guo M, Wei Z, et al. Determination of the optimal tilt angle of solar collectors for different climates of China. *Sustain* 2016; 8: 1–16.

34   Lowhorn GL. Qualitative and Quantitative Research: How to Choose the Best Design. *Pap Present Acad Bus World Int Conf* 2007; 1–5.

35   VTT Technical Research Centre of Finland LTD. LIWE facades_modules-to Metropolia_6-2017. 2017.

36   European Commission. JRC Photovoltaic Geographical Information System (PVGIS), http://re.jrc.ec.europa.eu/pvg_tools/en/tools.html (accessed 15 October 2018).

37   Variance Inflation Factor - Statistics How To, https://www.statisticshowto.datasciencecentral.com/variance-inflation-factor/ (accessed 19 November 2018).

38   Correlation analysis, http://pages.intnet.mu/cueboy/education/notes/statistics/pearsoncorrel.pdf (accessed 18 December 2018).

Appendices

Appendix I American Physical Society Reuse and Permissions License I
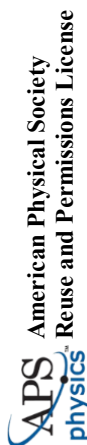
American Physical Society
Reuse and Permissions License

12-Oct-2018

This license agreement between the American Physical Society ("APS") and Khanh Dao ("You") consists of your license details and the terms and conditions provided by the American Physical Society and SciPris.

Licensed Content Information

License Number:	RNP/18/OCT/008477
License date:	12-Oct-2018
DOI:	10.1103/PhysRevB.75.115327
Title:	Offset energies at organic semiconductor heterojunctions and their influence on the open-circuit voltage of thin-film solar cells
Author:	Barry P. Rand, Diana P. Burk, and Stephen R. Forrest
Publication:	Physical Review B
Publisher:	American Physical Society
Cost:	USD $ 0.00

Request Details

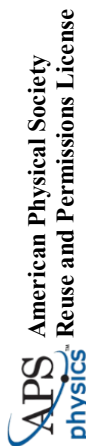|	
Does your reuse require significant modifications:	No
Specify intended distribution locations:	Finland
Reuse Category:	Reuse in a thesis/dissertation
Requestor Type:	Student
Items for Reuse:	Figures/Tables
Number of Figure/Tables:	1
Figure/Tables Details:	Open-circuit voltage (VOC) versus T for various donor-acceptor heterojunctions.
Format for Reuse:	Electronic

Information about New Publication:

University/Publisher:	Metropolia University of applied sciences
Title of dissertation/thesis:	The environmental test of organic photovoltaic panels
Author(s):	Dao Le Cam Khanh
Expected completion date:	Dec. 2018

License Requestor Information

Name:	Khanh Dao
Affiliation:	Individual
Email Id:	camkhanhdao@gmail.com
Country:	Finland

Page 1 of 2

American Physical Society
Reuse and Permissions License

TERMS AND CONDITIONS

The American Physical Society (APS) is pleased to grant the Requestor of this license a non-exclusive, non-transferable permission, limited to Electronic format, provided all criteria outlined below are followed.

1. You must also obtain permission from at least one of the lead authors for each separate work, if you haven't done so already. The author's name and affiliation can be found on the first page of the published Article.

2. For electronic format permissions, Requestor agrees to provide a hyperlink from the reprinted APS material using the source material's DOI on the web page where the work appears. The hyperlink should use the standard DOI resolution URL, http://dx.doi.org/{DOI}. The hyperlink may be embedded in the copyright credit line.

3. For print format permissions, Requestor agrees to print the required copyright credit line on the first page where the material appears: "Reprinted (abstract/excerpt/figure) with permission from [(FULL REFERENCE CITATION) as follows: Author's Names, APS Journal Title, Volume Number, Page Number and Year of Publication.] Copyright (YEAR) by the American Physical Society."

4. Permission granted in this license is for a one-time use and does not include permission for any future editions, updates, databases, formats or other matters. Permission must be sought for any additional use.

5. Use of the material does not and must not imply any endorsement by APS.

6. APS does not imply, purport or intend to grant permission to reuse materials to which it does not hold copyright. It is the requestor's sole responsibility to ensure the licensed material is original to APS and does not contain the copyright of another entity, and that the copyright notice of the figure, photograph, cover or table does not indicate it was reprinted by APS with permission from another source.

7. The permission granted herein is personal to the Requestor for the use specified and is not transferable or assignable without express written permission of APS. This license may not be amended except in writing by APS.

8. You may not alter, edit or modify the material in any manner.

9. You may translate the materials only when translation rights have been granted.

10. APS is not responsible for any errors or omissions due to translation.

11. You may not use the material for promotional, sales, advertising or marketing purposes.

12. The foregoing license shall not take effect unless and until APS or its agent, Aptara, receives payment in full in accordance with Aptara Billing and Payment Terms and Conditions, which are incorporated herein by reference.

13. Should the terms of this license be violated at any time, APS or Aptara may revoke the license with no refund to you and seek relief to the fullest extent of the laws of the USA. Official written notice will be made using the contact information provided with the permission request. Failure to receive such notice will not nullify revocation of the permission.

14. APS reserves all rights not specifically granted herein.

15. This document, including the Aptara Billing and Payment Terms and Conditions, shall be the entire agreement between the parties relating to the subject matter hereof.

Page 2 of 2

Appendix I American Physical Society Reuse and Permissions License II

American Physical Society Reuse and Permissions License

12-Oct-2018

This license agreement between the American Physical Society ("APS") and Khanh Dao ("You") consists of your license details and the terms and conditions provided by the American Physical Society and SciPris.

Licensed Content Information

License Number:	RNP/18/OCT/008478
License date:	12-Oct-2018
DOI:	10.1103/PhysRevB.82.245207
Title:	Recombination in polymer-fullerene bulk heterojunction solar cells
Author:	Sarah R. Cowan, Anshuman Roy, and Alan J. Heeger
Publication:	Physical Review B
Publisher:	American Physical Society
Cost:	USD $ 0.00

Request Details

Does your reuse require significant modifications:	No
Specify intended distribution locations:	Finland
Reuse Category:	Reuse in a thesis/dissertation
Requestor Type:	Student
Items for Reuse:	Figures/Tables
Number of Figure/Tables:	1
Figure/Tables Details:	(Color) Intensity dependence of Vbi, the voltage where the photocurrent=0
Format for Reuse:	Electronic

Information about New Publication:

University/Publisher:	Metropolia University of Applied Sciences
Title of dissertation/thesis:	The environmental test of Organic Photovoltaic cells
Author(s):	Dao Le Cam Khanh
Expected completion date:	Dec. 2018

License Requestor Information

Name:	Khanh Dao
Affiliation:	Individual
Email Id:	camkhanhdao@gmail.com
Country:	Finland

Page 1 of 2

American Physical Society Reuse and Permissions License

TERMS AND CONDITIONS

The American Physical Society (APS) is pleased to grant the Requestor of this license a non-exclusive, non-transferable permission, limited to Electronic format, provided all criteria outlined below are followed.

1. You must also obtain permission from at least one of the lead authors for each separate work, if you haven't done so already. The author's name and affiliation can be found on the first page of the published Article.

2. For electronic format permissions, Requestor agrees to provide a hyperlink from the reprinted APS material using the source material's DOI on the web page where the work appears. The hyperlink should use the standard DOI resolution URL, http://dx.doi.org/{DOI}. The hyperlink may be embedded in the copyright credit line.

3. For print format permissions, Requestor agrees to print the required copyright credit line on the first page where the material appears: "Reprinted (abstract/excerpt/figure) with permission from [FULL REFERENCE CITATION] as follows: Author's Names, APS Journal Title, Volume Number, Page Number and Year of Publication.] Copyright (YEAR) by the American Physical Society."

4. Permission granted in this license is for a one-time use and does not include permission for any future editions, updates, databases, formats or other matters. Permission must be sought for any additional use.

5. Use of the material does not and must not imply any endorsement by APS.

6. APS does not imply, purport or intend to grant permission to reuse materials to which it does not hold copyright. It is the requestor's sole responsibility to ensure the licensed material is original to APS and does not contain the copyright of another entity, and that the copyright notice of the figure, photograph, cover or table does not indicate it was reprinted by APS, with permission from another source.

7. The permission granted herein is personal to the Requestor for the use specified and is not transferable or assignable without express written permission of APS. This license may not be amended except in writing by APS.

8. You may not alter, edit or modify the material in any manner.

9. You may translate the materials only when translation rights have been granted.

10. APS is not responsible for any errors or omissions due to translation.

11. You may not use the material for promotional, sales, advertising or marketing purposes.

12. The foregoing license shall not take effect unless and until APS or its agent, Aptara, receives payment in full in accordance with Aptara Billing and Payment Terms and Conditions, which are incorporated herein by reference.

13. Should the terms of this license be violated at any time, APS or Aptara may revoke the license with no refund to you and seek relief to the fullest extent of the laws of the USA. Official written notice will be made using the contact information provided with the permission request. Failure to receive such notice will not nullify revocation of the permission.

14. APS reserves all rights not specifically granted herein.

15. This document, including the Aptara Billing and Payment Terms and Conditions, shall be the entire agreement between the parties relating to the subject matter hereof.

Page 2 of 2

Appendix II Three different suggested levels of outdoor testing

**Table 3**
The three different suggested levels of outdoor testing.

|		ISOS-O-1 (outdoor)	ISOS-O-2 (outdoor)	ISOS-O-3 (outdoor)
Test Setup	Light source	Direct sunlight in outdoor conditions. Choose a place away from possible shadows	Direct sunlight in outdoor conditions. Choose a place away from possible shadows	Direct sunlight in outdoor conditions. Choose a place away from possible shadows
	Mounting	Static: front side oriented towards the equator, at latitude angle. Tracking: front side facing sun	Static: front side oriented towards the equator, at latitude angle. Tracking: front side facing sun	Static: front side oriented towards the equator, at latitude angle. Tracking: front side facing sun
	Load (refer to Section 3.9)	MPP tracking—preferred. Open circuit—optional	MPP tracking—preferred. Open circuit—optional	MPP (resistor, passive) or MPP tracking (active)
	Temperature	Ambient	Ambient	Ambient
	R.H.	Ambient	Ambient	Ambient
	Characterization light source	Inside with simulated light	Outside under sunlight	Outside regularly and inside at certain periods
Testing protocol	Temp./R.H.	Monitor ambient values	Monitor NOCT and ambient R.H.	Monitor NOCT and ambient R.H.
	Solar irradiance (in W/m^2) and irradiation (in MJ/m^2)	Monitor irradiance and calculate accumulated irradiation	Monitor irradiance and calculate accumulated irradiation	Monitor irradiance and calculate accumulated irradiation
	JV characterization	Refer to Section 3.8	Refer to Section 3.8	Refer to Section 3.8
	Min. measurement intervals	Daily to weekly (adjust to device performance)	1/15 min–1/1 h recommended to establish variations across the day	Outside: 1/15 min–1/1 h to establish variations across the day; Inside: weekly or monthly
	Characterization temperature	Monitor specimen temperature on backside	Monitor specimen temperature on backside	Monitor specimen temperature on backside
	Characterization irradiance level	Monitor	Monitor irradiance	Monitor irradiance
	Wind monitoring	Optional	Optional	Monitor wind speed down to 0.25 m/s. The system should be installed ca. 1.2 m to the east or west of the devices under test and 0.7 m higher
	IPCE (at T_0, T_{80}, T_s, T_{s80} see Section 4.1)	Optional	Optional	Measure
	Note data taken in ranges	Optional	Ambient temperature outside of range 20 ± 15 °C. Irradiance below 400 W/m^2	Ambient temperature outside of range 20 ± 15 °C. Irradiance below 400 W/m^2. Wind speeds outside of range 1 ± 0.75 m/s. For 10 min following wind speeds exceeding 4 m/s. Wind direction within $\pm 20°$ east or west
Output	Location/time	Report latitude, longitude and date	Report latitude, longitude and date	Report latitude, longitude and date
	Irradiance and irradiation	Refer to Section 3.2.2	Refer to Section 3.2.2	Refer to Section 3.2.2
	Exposure temp./R.H.	Report ambient values	Report NOCT and R.H.	Report NOCT and R.H.
	Instantaneous performance parameters	Report J_{sc} and V_{oc} (FF and PCE/MPP and/or full JVs if possible)	Report J_{sc}, V_{oc}, FF, PCE/MPP; JVs optional	Report J_{sc}, V_{oc}, FF, PCE/MPP; JVs optional
	Stability performance parameters	Refer to Section 4	Refer to Section 4	Refer to Section 4
	Characterization light source	Report type and irradiance level	Report sunlight irradiance	Report type and irradiance level
	Wind	Optional	Optional	Report
	IPCE	Optional	Optional	Report
	Description of measurement protocol and setup	Report	Report	Report
	Load type	Report	Report	Report
Required equipment	Characterization light source	Solar simulator (close to AM1.5G)	Sunlight under clear sky conditions	Sunlight under clear sky conditions and solar simulator with AM1.5G
	Temperature monitoring	Ambient temperature measuring unit	RTD preferred, other device with ± 2 °C acceptable	RTD preferred, other device with ± 2 °C acceptable
	R.H. monitoring	Ambient R.H. measuring unit	Sensor with $\pm 5\%$ capability	Sensor with $\pm 5\%$ capability
	Irradiance monitoring	Pyranometer and/or photodiode	Irradiance monitoring unit (for example, pyranometer)	Matched photodiode for solar simulator and sunlight irradiance monitoring unit (for example, pyranometer)
	Load	Refer to Section 3.9	Refer to Section 3.9	Refer to Section 3.9
	Fixture	Tracking system preferred, stationary acceptable; bottom edge > 0.6 m above horizontal surface	Tracking system preferred, stationary acceptable; bottom edge > 0.6 m above horizontal surface	Tracking system preferred, stationary acceptable; bottom edge > 0.6 m above horizontal surface
	Wind monitoring	Optional	Optional	Required, weather station

Appendix II Additional plots of V_OC versus Temp. plots at different Irradiation level
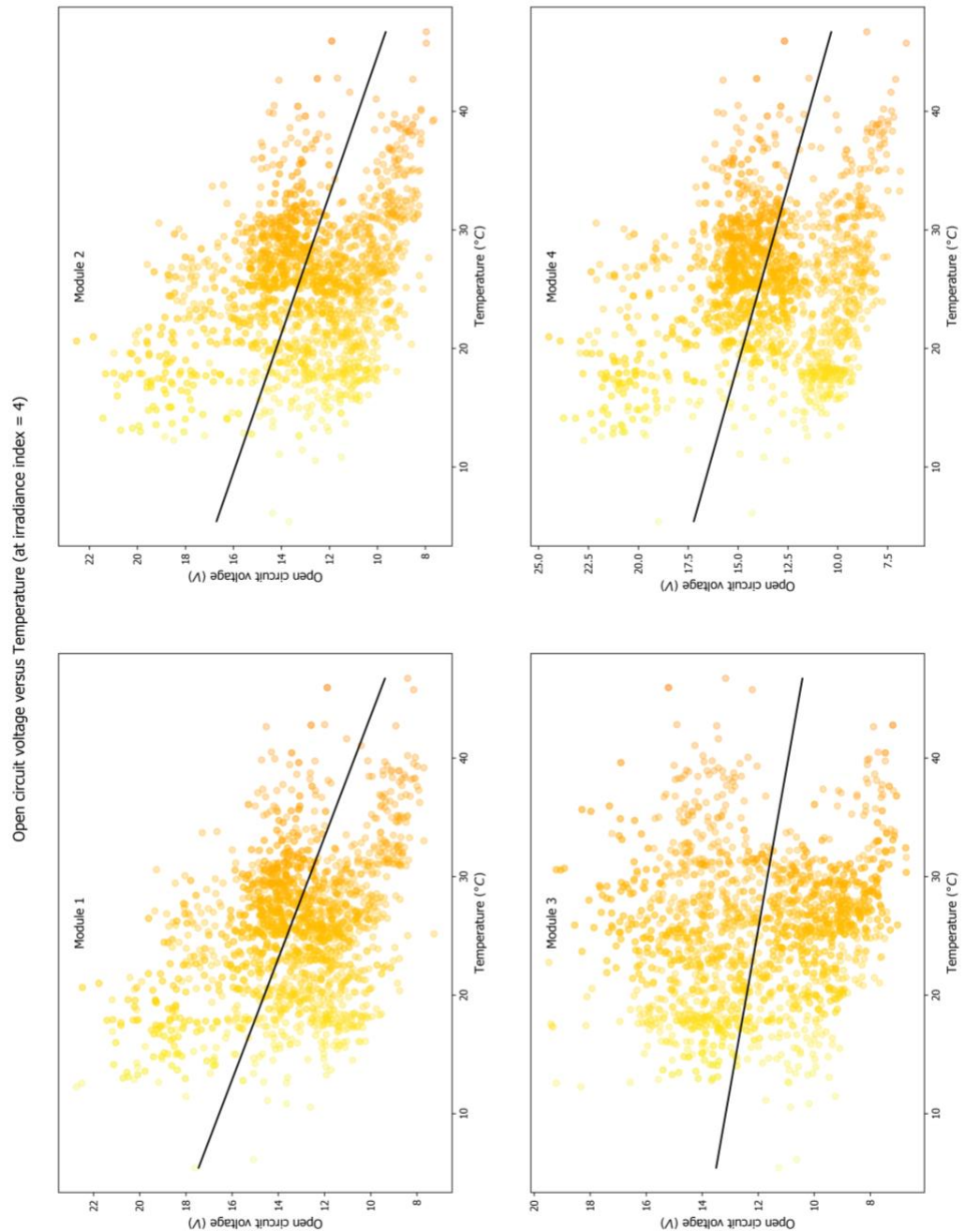
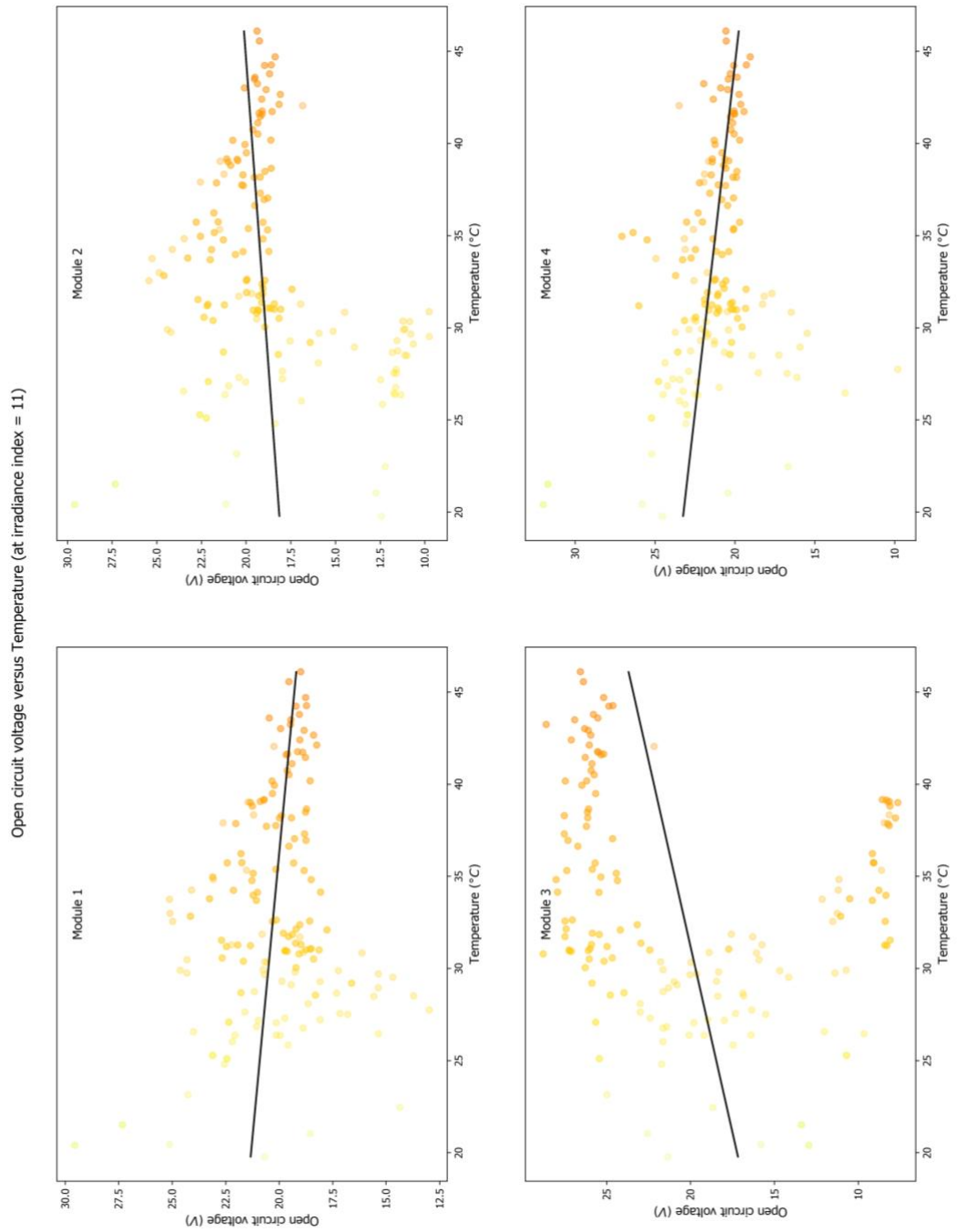

Irradiation index = 4 means the 40mW/cm^2 irradiation level

Open circuit voltage versus Temperature (at irradiance index = 9)
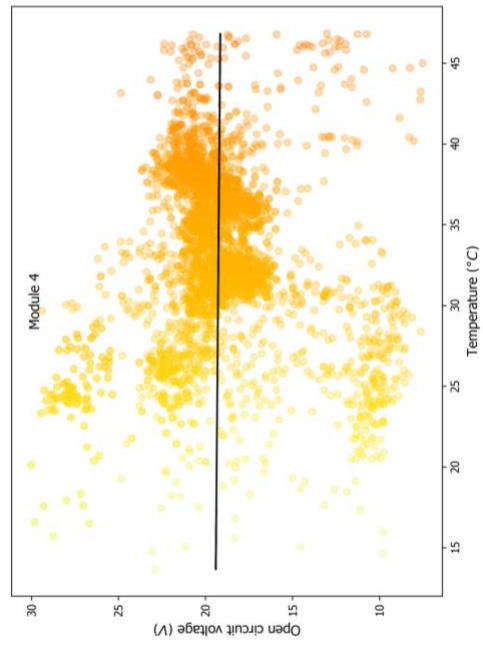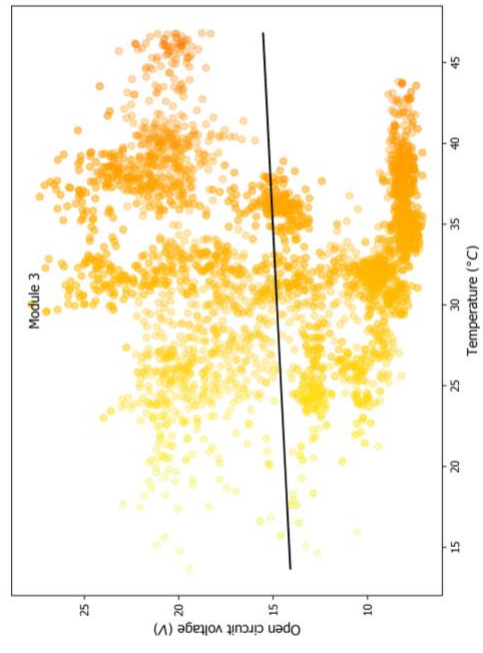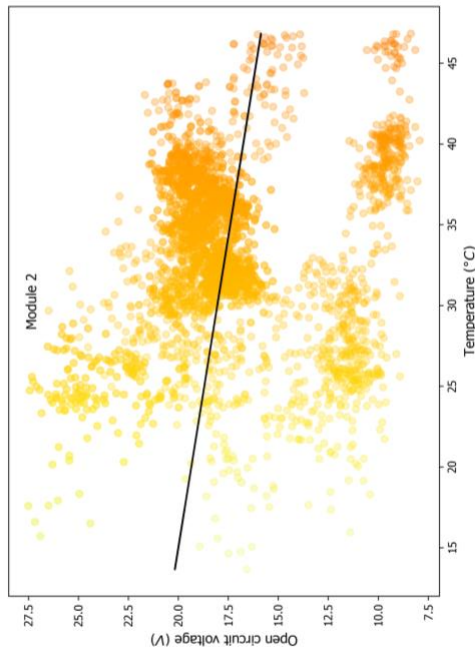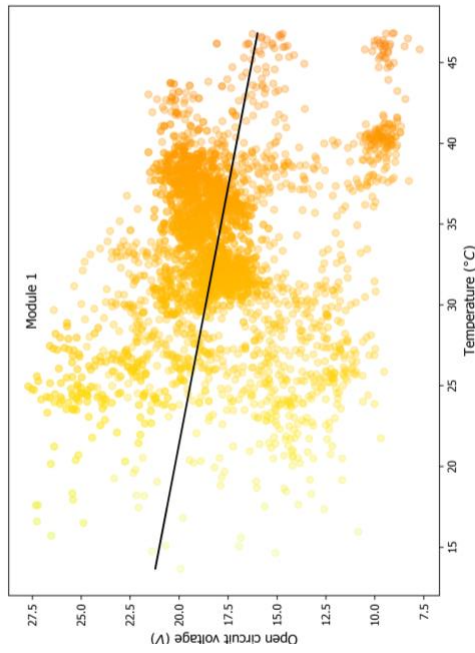
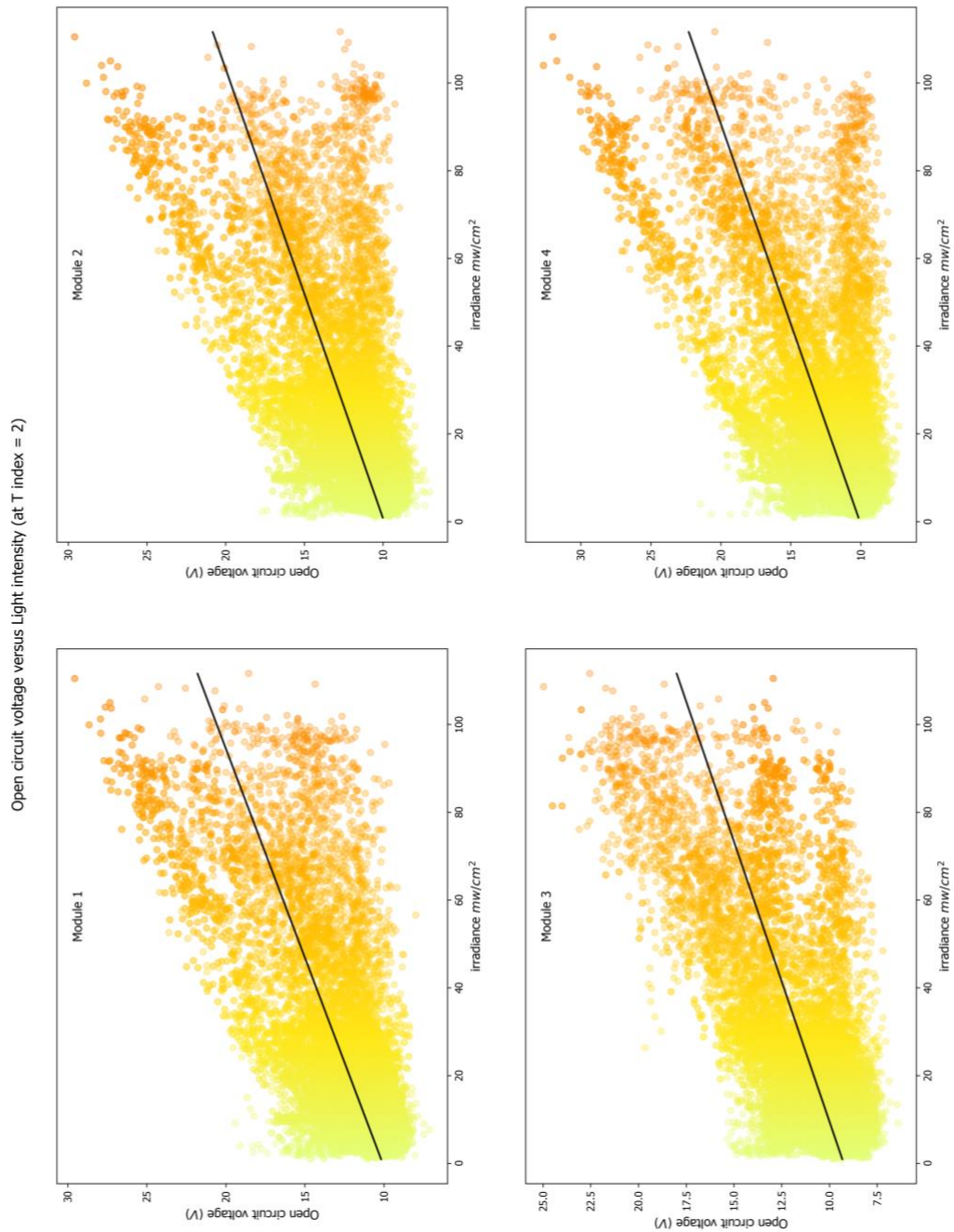Irradiation index = 9 means the 90mW/cm^2 irradiation level

Open circuit voltage versus Temperature (at irradiance index = 11)

Irradiation index = 11 means the 110mW/cm^2 irradiation level

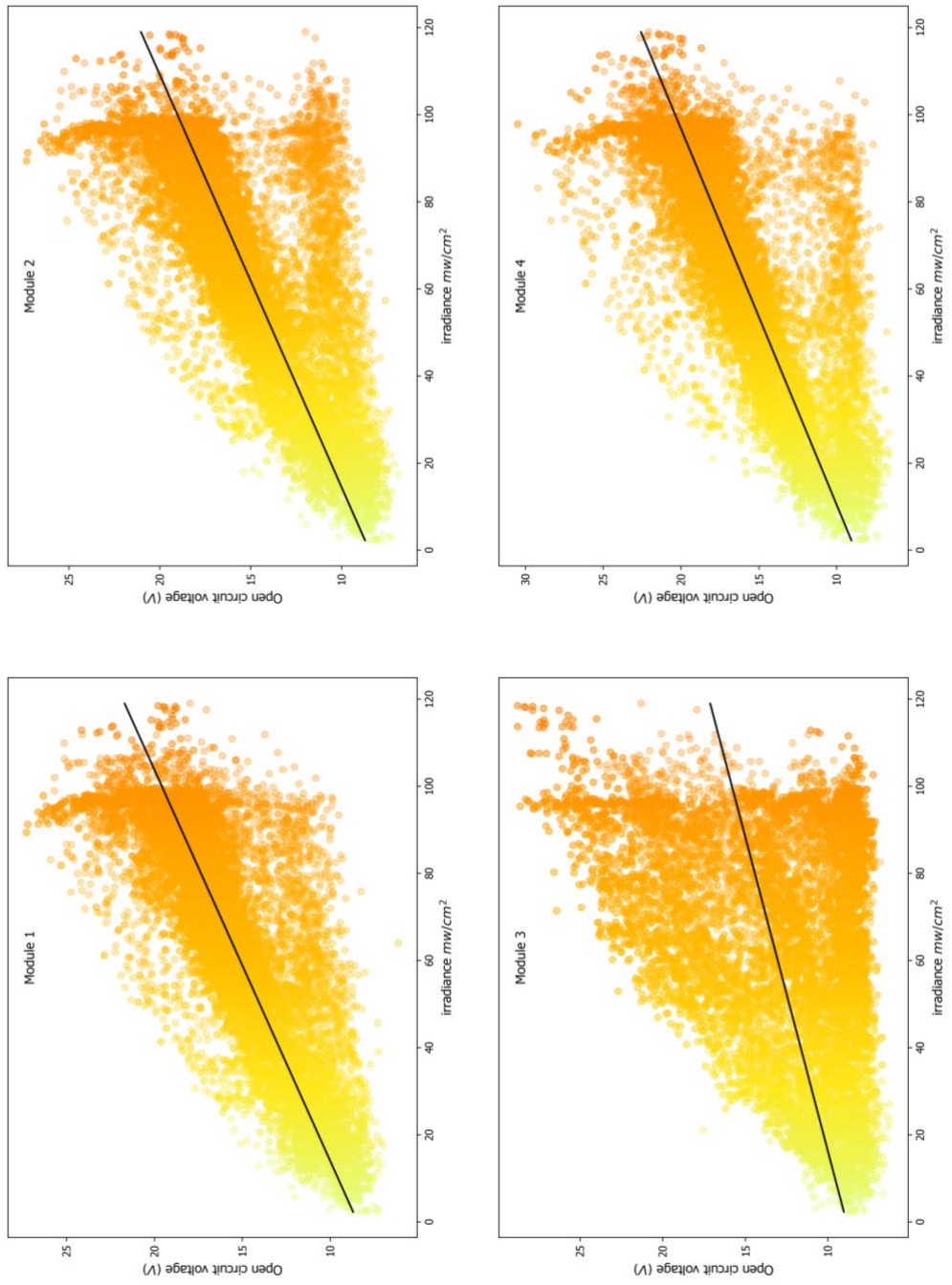**Appendix IV Additional plots of V_{OC} versus Irradiation plots at different Temp. level**

T index = 2 means ambient Temperature = 20°C

Open circuit voltage versus Light intensity (at T index = 3)

T index = 3 means ambient Temperature = 30°C